NTNU

Norwegian University of
Science and Technology

Study of the Particle Properties of Iron Oxide/Hydroxide Precipitate in Nickel Production

Mona Aufles Hines

Preface

The present thesis and experimental work is submitted to the Norwegian University of Science and Technology, Department of Chemical Engineering and Biotechnology and is a part of KP4900 - Chemical process technology, master thesis.

First of all I wish to thank my supervisor Professor Jens-Petter Andreassen and Co-supervisor PhD Candidate Ina Beate Jenssen for giving me motivation and theoretical guidance. I would also like to thank Senior Specialist (R&D) Oluf Bøckman and Senior Specialist (Hydrometallurgy) Ole Morten Dotterud at Glencore for theoretical and practical guidance.

I am also grateful to Laboratory Engineer Liv Carlhamn Rasmussen at Elkem for help with Powder X-ray Diffraction analysis, and Postdoctoral Fellow Xiaoguang Ma for instrumental help at NTNU. Laborants Kent Skaiaa and Tore Amdal have also been very helpful during the stay at Glencore.

Trondheim, 3rd of July 2017

Mona A. Hines

Abstract

The background for this thesis was crystallization of iron in nickel production at Glencore and a review of filterability properties of iron oxide/hydroxide precipitate. The nickel plant in Kristiansand produces nickel and cobalt by a chlorine leaching process with chloride electrowinning. Copper is produced by sulphate electrowinning. The aim of this thesis was to determine how different temperatures and supersaturation, due to residence time, affected the crystalline type and filterability of iron oxide/hydroxide precipitate.

Precipitation of iron oxide/hydroxide using divalent iron chloride were performed in a continuous system at 29, 65 and 79°C with varying residence time. Sodium hydroxide was used as a base and hydrogen peroxide was added to oxidize the divalent iron. Supersaturation is mainly determined by pH and affect the crystal phase and size of the particles which are obtained. During a three week stay at Glencore experiments at 30, 65 and 90°C were performed with solution from their process as feed material. Nickel carbonate and chlorine gas were used as base and oxidizing agent, respectively.

The oxidation/reduction potential and pH were monitored during the experiments and the oxidation ratio was measured with Ultraviolet–visible spectrophotometer (UV-Vis). The filterability were examined using a BHS filtration unit, type of precipitation was determined by Powder X-ray Diffraction (PXRD) analysis and the particles were visually examined by using Scanning Electron Microscope (SEM).

At NTNU the precipitate was found to be ferrihydrite but a clear correlation between filterability, temperature and residence time could not be ascertained. Akaganeite was obtained for all the experiments at Glencore both for using process solution and divalent iron chloride as feed material. The filterability were improved both with increasing temperature and longer residence time, where the residence time had a higher impact than the temperature.

Sammendrag

Bakgrunnen for denne oppgaven var krystallisering av jern i nikkelproduksjon ved Glencore og filtreringsegenskapene for jernoksid/hydroksid. Nikkelverket i Kristiansand produserer nikkel, kobolt og kobber ved elektrolyse. Målet med denne oppgaven var å bestemme hvordan ulik temperatur og overmetning, basert på oppholdstid, påvirket type og filtrerbarhet av jernoksid/hydroksid-utfellinger.

Utfelling av jernoksid/hydroksid ved bruk av toverdig jernklorid ble utført i et kontinuerlig system ved 29, 65 and 79°C med varierende oppholdstid. Natriumhydroksid ble anvendt som base og hydrogenperoksid ble tilsatt for å oksidere toverdig jern. Overmetningen bestemmes hovedsakelig av pH og påvirker krystallfase og størrelse av partiklene som blir dannet. Gjennom et tre-ukers opphold ved Glencore ble forsøk ved 30, 65 and 90°C utført med løsning fra deres prosess som fødemateriale. Nikkelkarbonat og klorgass ble anvendt som henholdsvis base og oksidasjonsmiddel.

Redox (reduksjon–oksidasjon) potensialet og pH ble loggført under forsøkene og oksidasjonsforholdet ble målt med ultrafiolett spektrofotometer (UV-Vis). Filtrerbarheten ble undersøkt ved hjelp av en BHS-filtreringskolonne, type utfelling ble bestemt ved røntgendiffraksjon (PXRD) og partiklene ble visuelt undersøkt ved bruk av elektron-mikroskopi (SEM).

Ved NTNU ble det produsert ferrihydritt og det ble det ikke sett noen klar sammenheng mellom filtrerbarhet, temperatur og oppholdstid. Akaganeitt ble dannet for alle forsøkene ved Glencore både ved bruk av prosessløsning og toverdig jernklorid som fødemateriale. Filtrerbarheten ble forbedret både ved med økende temperatur og lengre oppholdstid, hvor oppholdstiden hadde størst innvirkning.

Contents

List of Figures

List of Tables

1   Introduction

The background for this thesis was crystallization of iron in nickel production at Glencore and the filterability properties of iron oxide/hydroxide precipitate. The nickel plant in Kristiansand produces nickel and cobalt by a chlorine leaching process with chloride electrowinning. Copper is produced by sulphate electrowinning [6].

The aim of this thesis was to determine how different temperatures and supersaturation, due to residence time, affected the crystalline type and filterability of iron oxide/hydroxide precipitate. Precipitation of iron oxide/hydroxide using divalent iron chloride were performed in a continuous system at 29, 65 and 79°C with varying residence time. Sodium hydroxide was used as a base and hydrogen peroxide was added to oxidize the divalent iron. Supersaturation is mainly determined by pH and affect the crystal phase and size of the particles which are obtained. During a three week stay at Glencore the experiments were performed at 30, 65 and 90°C with feed material from their process. Nickel carbonate and chlorine gas were used as base and oxidizing agent, respectively.

The redox (reduction–oxidation) potential and pH were monitored during the experiments and the oxidation ratio was measured using an Ultraviolet–visible spectrophotometer (UV-Vis). The filterability were examined by using a BHS filtration unit, type of precipitation was determined by Powder X-ray Diffraction (PXRD) analysis and the particles were visually examined by using Scanning Electron Microscope (SEM).

2   Theoretical Background

2.1   Glencore Nickel Refinery in Norway

Glencore in Kristiansand produces nickel, copper, sulfuric acid and platinum-group metals with matte from Canada and Botswana as feed material. The process is presented in Figure 2.1 [1], where the red area is of interest for this thesis. Glencore wants to utilize complex primary or secondary feed materials in a larger scale, which leads to high priority of removing impurities like iron [6].

Slurry from the autoclave leaching undergoes pre-precipitation to remove copper, followed by washing and filtrating to reduce the amount of chloride. The content is 220 g/L nickel, 11 g/L cobalt, 7 g/L iron and 0.5 g/L copper [1]. Iron is then removed by a "Fe-II precipitation step" by oxidizing Fe^{2+} to Fe^{3+} using chlorine gas, see Equation 1. The hydrolysis of ferric ions occurs simultaneously according to Equation 2, neutralized by nickel carbonate in Equation 3 [6][1].

$$2FeCl_2 + Cl_{2(g)} \rightarrow 2FeCl_3 \tag{1}$$

$$2FeCl_3 + H_2O \rightarrow 2Fe(OH)_{3(s)} + 6HCl \tag{2}$$

$$6HCl + 3NiCO_{3(s)} \rightarrow 3NiCl_2 + 3H_2O + 3CO_{2(g)} \tag{3}$$
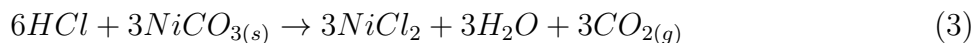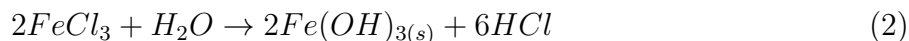
Normally the feed stream contains 7-15 g/L of iron [6]. Based on this the amount of iron for the experimental part of this thesis was chosen to 10 g/L.
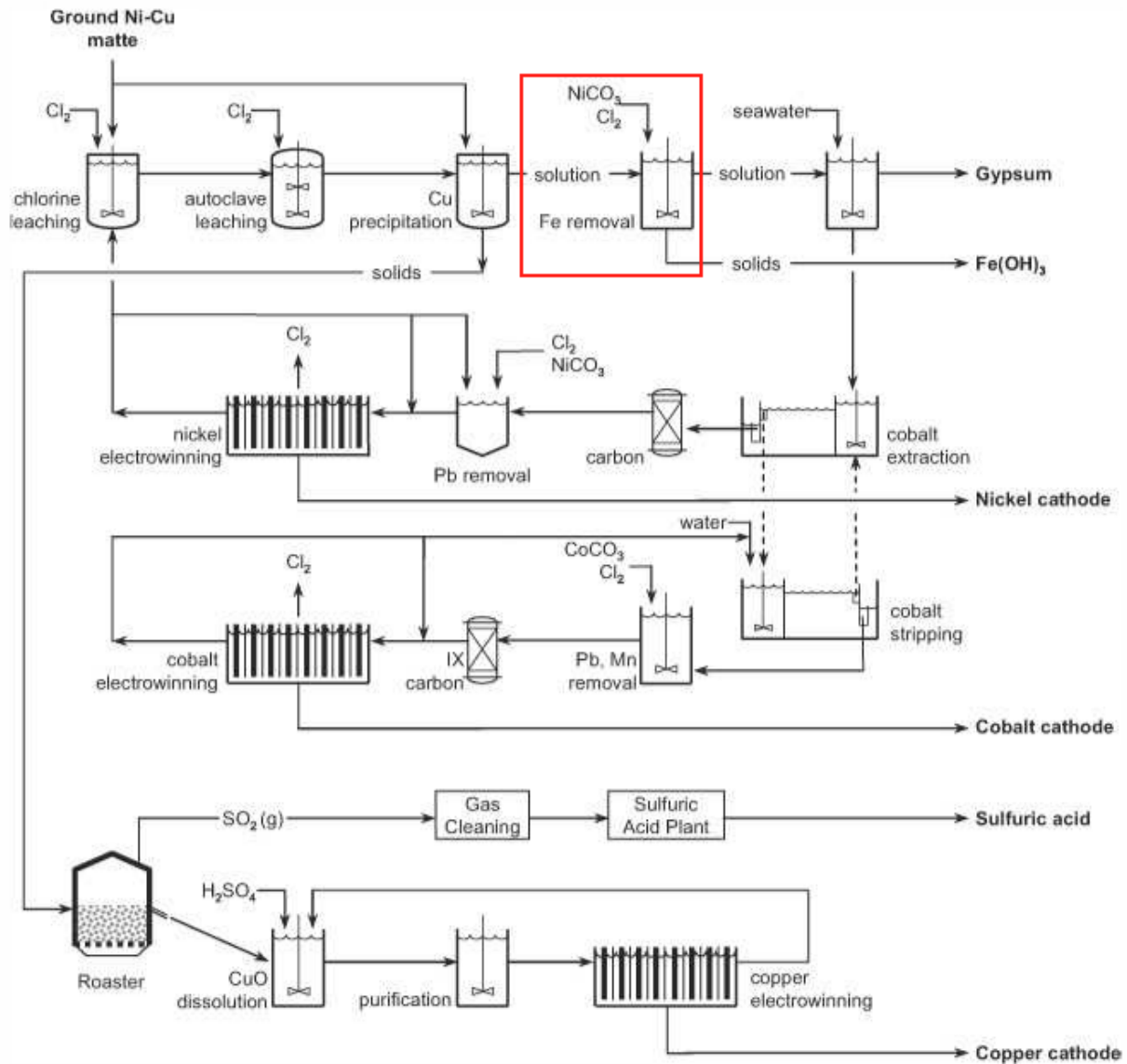
Figure 2.1: Flowsheet over the nickel refining process at Glencore in Kristiansand. The area in red is of interest for this thesis [1].

2.2 Crystallization and Supersaturation

Crystallization from solution occurs through creation of new crystals, known as nucleation, followed by growth to larger crystals [3][7]. At a specific temperature the saturation point for a solution is when the amount of solute and solvent is equal [8]. When there is more dissolved solid than required for obtaining a thermodynamic equilibrium the solution is supersaturated (oversaturated), which is required for a crystallization process to

occur [8][7][9]. With an increasing number of crystals the supersaturation is decreasing and by controlling the temperature crystals of specific types can be obtained [10].

The supersaturation for electrolytes of aqueous solutions which are sparingly soluble is expressed by Equation 4. IAP is the ion activity product and Ksp is the activity solubility product. a_+ [mol/L] and a_- [mol/L] is the cation and anion ionic activity and v is the sum of mole ions in one mole solute [8].

$$S = \left(\frac{IAP}{Ksp}\right)^{\frac{1}{v}} = \left(\frac{(a_+)^{v+} \cdot (a_-)^{v-}}{Ksp}\right)^{\frac{1}{v}} \tag{4}$$

2.3 Nucleation

In addition to supersaturation a solution have to contain a certain concentration of solids in order to initiate a crystallization process. Primary nucleation is a spontaneous process where active crystals are absent at the beginning of the nucleation. Primary heterogeneous nucleation have non-active particles present before nucleation and primary homogeneous nucleation does not contain any kind of particles before nucleation [8][3][7].

2.3.1 Primary Homogenous Nucleation

After the molecules/ions have resisted the tendency to redissolve in solution they are added to critical clusters giving nucleation and growth, where chains and monolayers are providing the base of a crystalline structure. Further development of the structure is occurring in regions with high supersaturation making the nucleus grow beyond a critical size. The size of a crystal determines how a new crystalline lattice in a supersaturated solution behaves. Particles smaller than the critical size will dissolve and larger particles will grow [8].

The nucleation rate, J [# nuclei/s·m^3], is given in Equation 5. k is the Boltzmann constant, T is the temperature [K], A is an independent kinetic parameter and $\Delta G_{crit.,homogen.}$ [J/mol] is the critical free energy for homogeneous nucleation which is maximized when the critical size of the particles is reached [8][11]. For a spherical nuclei Equation 6 is valid, where the

geometrical parameters for $\Delta G_{crit.,homogen.}$ is included. From the last equation it is clearer to point out that J is dependent of temperature, degree of supersaturation, S, and the interfacial tension, γ [8].

$$J = A \cdot exp\left(\frac{-\Delta G_{crit.,homogen.}}{k \cdot T} \right) \tag{5}$$

$$J = A \cdot exp\left[-\frac{16 \cdot \pi \cdot \gamma^3 \cdot v^2}{3 \cdot k^3 \cdot T^3 \cdot (lnS)^2} \right] \tag{6}$$

2.4   Crystal Growth and Transformation

After nucleation the nuclei that are stable grow to crystals of visible sizes. It is predicted that when a crystal is growing particles are continuously deposited on the surface with a rate proportional to the difference between the deposition and the bulk concentration. However, the effects of supersaturation have to be considered additionally. Surface diffusion is when particles are available to move over the crystal surface, obtaining a weak bounded adsorption layer at the interface which is significant for crystal growth. The attachment will occur at the surface positions with largest attractive forces. This will either continue until the plane is full or dislocations occur in the crystal surface, resulting in surface growth. Also in some cases random nucleation over the crystal surface is promoting growth of the crystals [8][3][11].

2.5   Iron Oxides

Iron can be oxidized to oxides, oxyhydroxides and hydroxides. The first crystalline phase is often metastable like polymorph or hydrate, which rapidly undergoes a reversible or irreversible transformation into a more stable phase [8]. All iron oxides consist of a basic structure of octahedral with one Fe ion surrounded by O or OH ions, differing in composition and crystal structure. Some examples with name, chemical formula, crystal system/shape and color are given i Table 2.1 [4][5].

Table 2.1: Examples of iron oxides and oxyhydroxides [3][4][5].

Name	Chemical formula	Type	Crystal system/shape	Color
Akaganeite	β-FeOOH	Oxyhydroxide	Tetragonal/rods	Yellow/brown
Ferrihydrite	$Fe_5HO_8 \cdot 4H_2O$	Oxides	Trigonal/spherical	Red/brown
Magnetite	Fe_3O_4	Oxides	Cubic/octahedral	Black
Hematite	α-Fe_2O_3	Oxides	Trigonal/hexaginal	Bright red

Ferrihydrite is generally the first product which is obtained and the particles are considered to be in the range of 3–7 nm, where agglomeration and aggregation may produce bulk particles up to 100 mm. This gives high surface area and a porous structure. Ferrihydrite is metastable and is easily transformed to more stable crystalline products [12][13].

In ferrihydrite, akaganeite and hematite the iron ion is trivalent. In order to obtain magnetite both di- and trivalent iron ions have to be present. In high chloride concentrations, at low pH and elevated temperatures (e.g. 60°C), akaganeite is often favored [4]. It is not an actual iron oxide since it contains structural chloride [14]. Akaganeite can be transformed into for instance goethite and hematite, where hematite is the most thermodynamically stable phase [15][16]. Akaganeite crystals are very small particles typically between 0.1-1 μm [13].

Hematite is generally produced at temperatures above 90°C. If a strong alkaline environment is obtained (5 M NaOH) temperatures down to 70°C can be sufficient. To form hematite there should be no presence of chloride due to the favoring of akaganeite formation. At temperatures around 100°C maksimum 0.02 M chloride can still form hematite [4].

2.5.1   Characterization

As described above, the size of iron oxide crystals are ranging from 0.01 to several μm. One of the most used characterization techniques are X-ray powder diffraction (XRD). The minimum size which is possible to diffract X-rays is 2-3 nm. Ferrihydrite has a very characteristic broad banded pattern in XRD, this due to a disordered compound that has short-range structural order where the occurrence of ferrihydrite often is limited to a rapid oxidation of Fe^{2+} [12][4].

2.5.2   Filterability

Particle size is important for filtration, washing and drying in the industry [7]. The crystal properties of the suspension which is filtrated are essential for the resistance, porosity and compressibility of the filter cake [17]. In general smaller particles tend to accumulate in the filter and makes the filtration more difficult.   Large spherical particles are therefore desirable [18][19][20].   Larger particles give less interactions at the particle–liquid interface [20].

2.6   Filtration

Solid particles can be separated from a liquid using filtration by deposition on a filter medium, called septum. This medium is mainly only permeable to the liquid phase, making the solid particles deposed on the surface or in depth of the septum. The permeability of the liquid phase is related to a pressure gradient, where the separated liquid is called filtrate. There will always be to some extent residual moisture in the filter cake and solids in the filtrate [21].

Filtration can be used for recovery of solids where the filtration often is followed by washing to eliminate liquid contaminants in the pores of the filter cake and further deliquoring and drying of the filter cake [21][22].

There are different classifications of filtration. In this thesis the focus is on filtration with constant pressure and deposing of particles on a filter paper, using nitrogen gas to obtain the desirable pressure. The rate of filtration decreases with increasing cake thickness when performing cake filtration. The solids are deposited as a homogeneous porous layer with constant permeability on the upstream side of the filter medium. After the first cake layer is formed further deposition of solids is on top of the first layer, where the filter medium only functions as support [21][22]. Figure 2.2 shows a schematic overview of cake filtration where the suspension is above the filter medium.
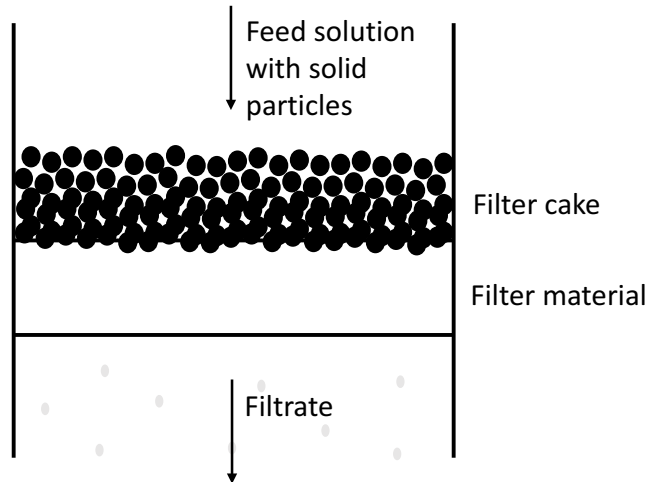
Figure 2.2: Cake filtration where the suspension is above the filter medium.

Suspensions with high solid concentration will mostly form "bridges" over the filter openings instead of the particles passing through the filter. This prevents clogging of the filter medium and gives a favorable filtration, where the desired concentration of solids may be assumed to be in excess of 1% by volume. The filtrate flows through due to the applied pressure, where the magnitude is proportional to the resistance obtained from the frictional drag force on the liquid as it passes through. Settling of solid particles by gravity often happen simultaneously as the filtration if the filtration is performed in the same direction as the gravity. For this thesis the suspension is above the filter medium and particle settling increases the kinetics of cake formation [22].

If the particles are easily deformed or rearranged under pressure, such as ferric hydroxide, the filter cake is compressible. With increasing pressure the cake porosity decreases and the hydraulic resistance to the liquid phase flow increases [22]. The formula for calculating the effective solid concentration, c $[g/cm^3]$, for a suspension resulting in a compressible filter cake, is given in Equation 7. Where s is the mass fraction of solids in the suspension, ρ_l $[g/cm^3]$ is the density of the filtrate, ρ_s $[g/cm^3]$ is the density of the solids and ϵ is the average porosity of the filter cake given in Equation 8 [23].

$$c = \frac{\rho_l}{\frac{1}{s} - \left(1 + \frac{\rho_l}{\rho_s} \cdot \frac{\epsilon}{(1-\epsilon)}\right)} \tag{7}$$

$$\epsilon = \frac{A \cdot h - \frac{m_s}{\rho_s}}{A \cdot h} \tag{8}$$

The porosity indicates how much the filter cake is compressed with respect to the volume that does not containing any solids, expressed by $\frac{m_s}{\rho_s}$. A $[cm^2]$ is the cross section area of the filter, h [cm] is the height of the filter cake and m_s [g] is the mass of the dry filter cake [23].

This leads to the most important parameter in cake filtration, the permeability of the cake presented by the specific cake resistance, α [cm/g]. When performing filtration with constant pressure Equation 9 can be used in order to calculate α [23][24].

$$\frac{t - t_i}{V - V_i} = \frac{\alpha \cdot c \cdot \mu}{2 \cdot A^2 \cdot \Delta p} \cdot (V + V_i) + \frac{\mu \cdot R}{A \cdot \Delta p} \tag{9}$$

Where $\frac{\alpha \cdot c \cdot \mu}{2 \cdot A^2 \cdot \Delta p}$ and $\frac{\mu \cdot R}{A \cdot \Delta p}$ are the slope and the intersection with the y-axis, respectively, when plotting $\frac{t - t_i}{V - V_i}$ by $(V + V_i)$. Δp [mPa] is the pressure difference and μ $[mPa \cdot s]$ is the viscosity of the filtrate [23][24].

3   Experimental

The experimental work will be presented during this section. For this thesis precipitation of iron oxide/hydroxide in a continuous system was examined. The aim of this thesis was to determine how different temperatures and supersaturation, with respect to residence time, affected the crystalline type and filterability of iron oxide/hydroxide precipitate.

The experiments were performed at 29, 65 and 79°C. Sodium hydroxide was used as a base and hydrogen peroxide was added to oxidize the divalent iron. Supersaturation is mainly determined by pH and affect the crystal phase and size of the particles which are obtained. During a three week stay at Glencore the experiments were performed at 30, 65 and 90°C with solution from their process as feed material. Nickel carbonate and chlorine gas were used as base and oxidizing agent, respectively.

Information of the applied chemicals and calculations of the amount are given in Appendix A and E, respectively. The procedures describing the filtration process and Ultraviolet–visible (UV-vis) determination in order to quantify the amount of iron, is described in Appendix F.

3.1   Equipment at NTNU

A continuous reactor (2000 mL), see Figure 3.1, with double glass walls was used with water circulation to adjust the temperature. Reflux of the condensate was obtained using a Liebig condenser. Redox (reduction–oxidation) potential and pH were measured using a Mettler Toledo Seven Excellence.

A. Redox-measurement
B. Water inlet (temp. control)
C. Double-walled vessel with heating jacket
D. Three inlets; divalent iron chloride, hydrogen peroxide, sodium hydroxide
E. Stirrer engine
F. Lid with openings for redox-electrode, pH-electrode, three inlets for solutions
G. pH-measurement
H. Outlet of suspension/product
I. Two baffles attached to the lid
J. Four-bladed impeller
K. Water outlet (temp. control)
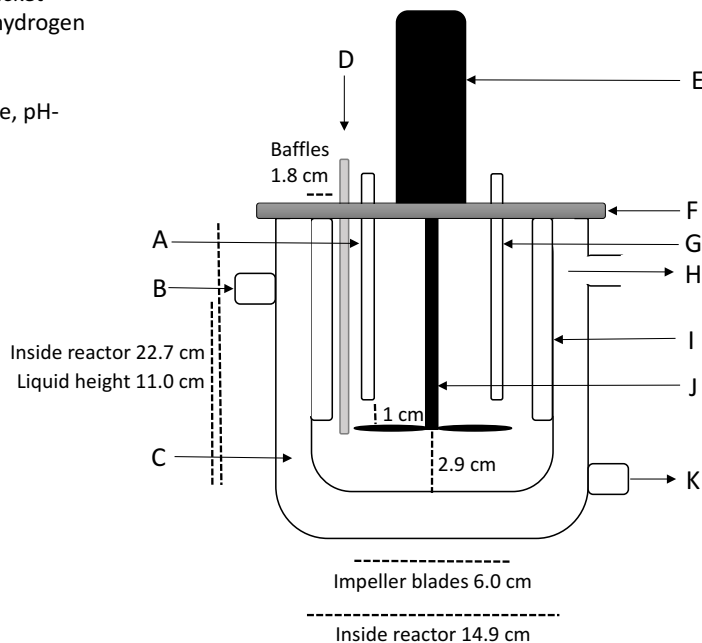
Figure 3.1: Sketch of the continuous reactor used for the experiments at NTNU.

The filterability of the precipitate was examined by a BHS filtration unit, see Figure 3.2. The oxidation ratio was measured using a Thermo Electron Spectronic Helios Alpha Beta UV-Vis Spectrophotometer. The type of iron precipitation was determined using D8 DaVinci Powder X-ray Diffraction (PXRD). The particles were visually examined by using Hitachi S-3400N Scanning Electron Microscope (SEM). The Visual MINTEQ computer software was used to obtain the activities for calculating the supersaturation for each experiment.
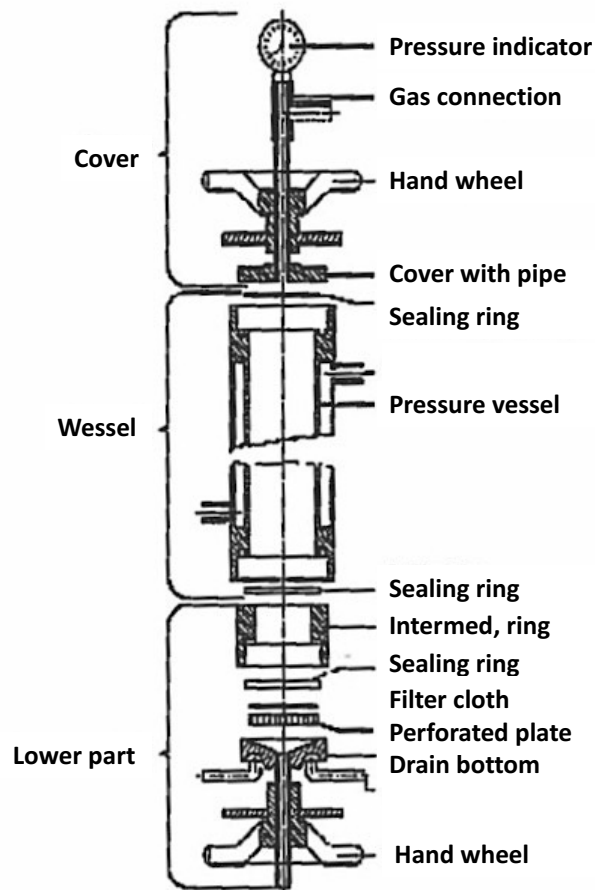
Figure 3.2: Sketch of the BHS filtration unit [2].

3.2   Experimental Procedure at NTNU

The total amount of iron for each experiment was chosen to be 10 g/L, based on the amount of iron in the feed material at Glencore (7-15 g/L), as mentioned in Section 2.1. Divalent iron chloride, sodium hydroxide and hydrogen peroxide were dissolved in three separate containers with distilled water. The solutions were mixed in the reactor using a mechanical stirrer with a four bladed impeller (450 rpm). The experimental setup is shown in Figure 3.3.

Each solution was pumped continuously into the reactor ensuring a constant pH and redox when reaching steady state. The experiments were performed with varying durations repeating the residence time (15 and 45 min). The suspension was filtered and the filter cakes were dried using a drying cabinet.
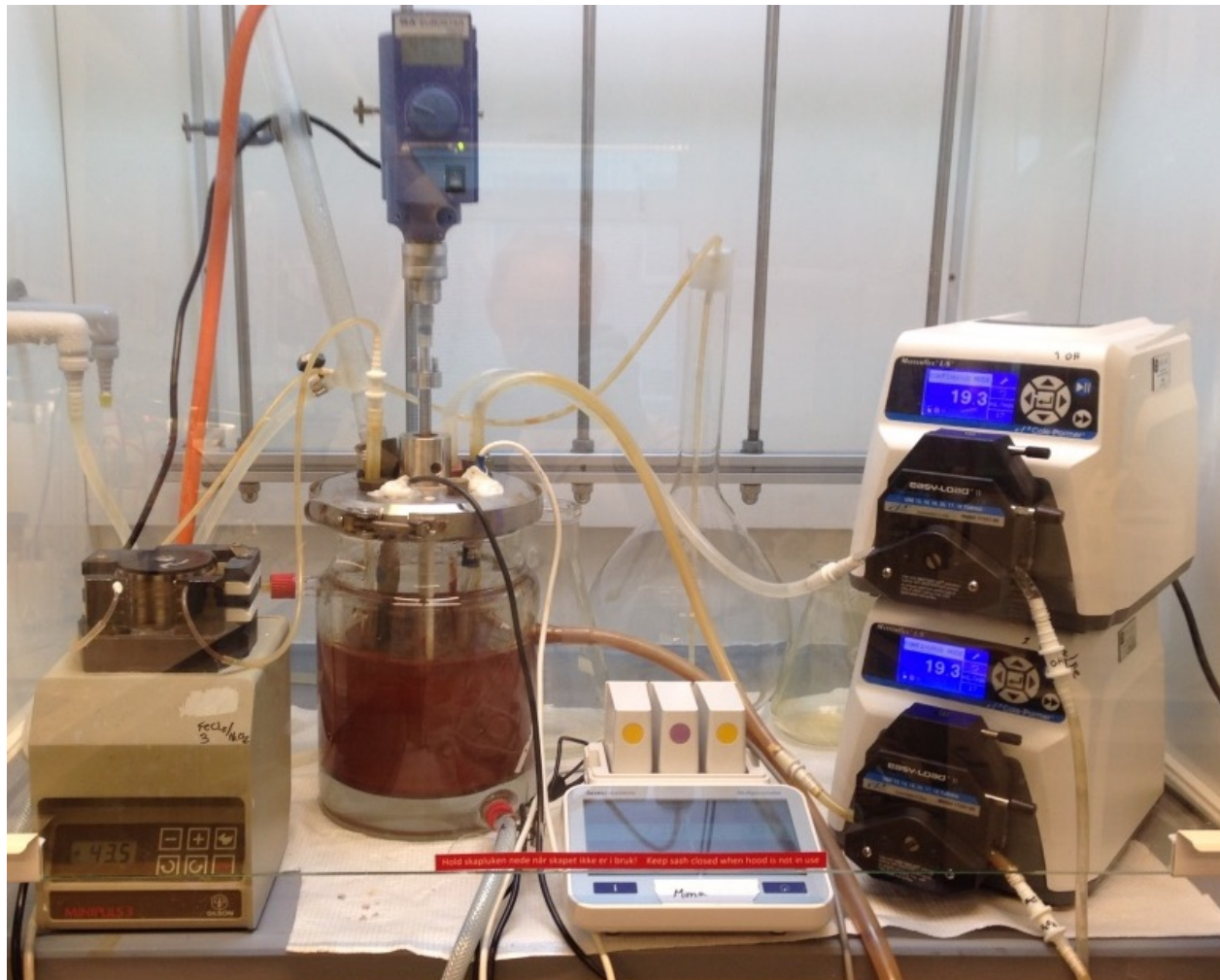
Figure 3.3: The experimental setup at NTNU.

3.3 Experimental Procedure at Glencore

Feed material and nickel carbonate from the process at Glencore was pumped into the reactor and chlorine gas was bubbled through the suspension. The suspension was mixed in the reactor using a mechanical stirrer (500 rpm). Desired set point for pH (pH 1.8) and redox (480 mV) used to adjust the pumping rate of nickel carbonate and chlorine gas was controlled by using the computer program LabRigg created by Terje Nygaard. The feed material was pumped at continuos rate. The experimental setup is shown in Figure 3.4.

The experiments were performed with varying durations repeating the residence time (45 and 75 min) 3 times. The suspension was filtered and the filter cakes were dried using a drying cabinet.
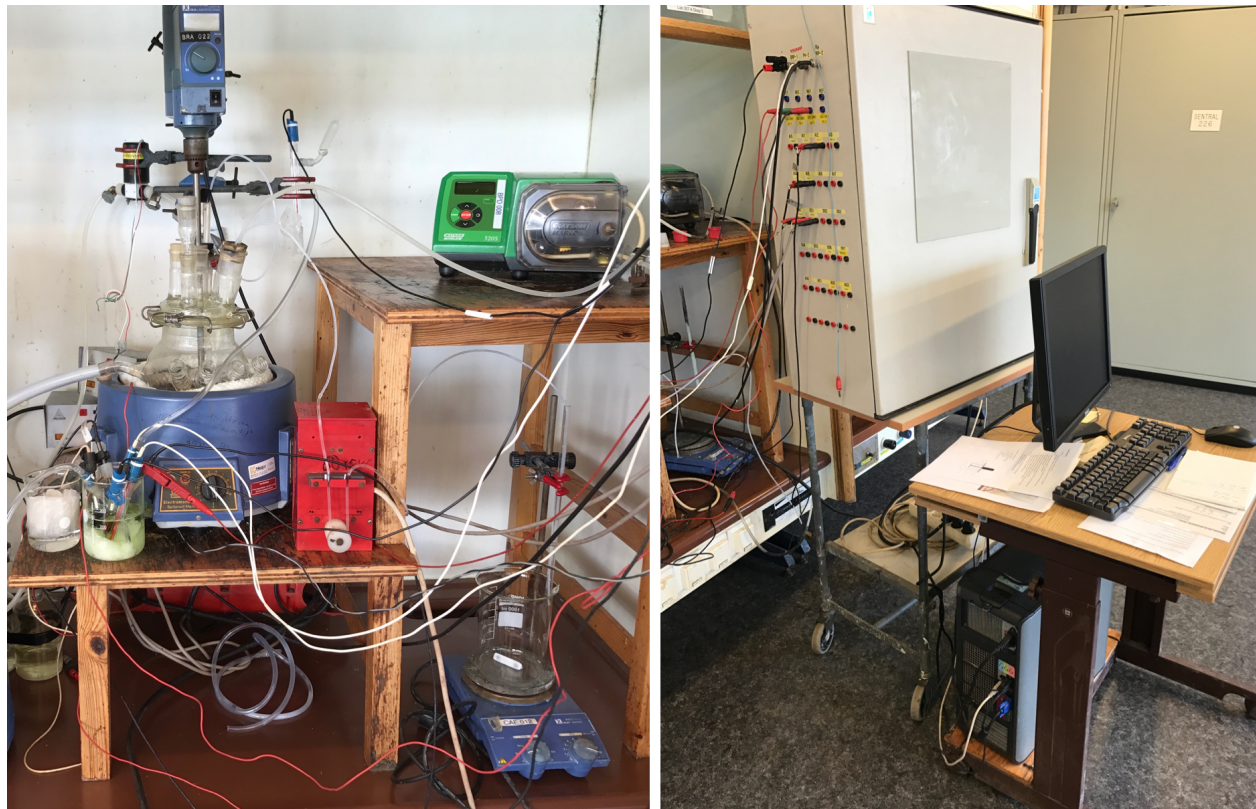
Figure 3.4: The experimental setup at Glencore with the computer logging used for feedback control.

4 Results and Discussion

The results from the experiments performed at NTNU and Glencore are presented and discussed during this section. The experiments performed at NTNU and Glencore are not compared due to various conditions associated with feed material, base solutions, oxidation agents and experimental setup. Both at NTNU and Glencore various test experiments were performed to learn how the different systems responded. However, these experiments are not presented during this thesis. Examples of calculations are given in Appendix E. All calculations for this thesis were done by using Excel.

4.1 Experiments at NTNU

The experiments at NTNU were performed to examine the effect of temperature and residence time on the filterability of iron oxide/hydroxide precipitate. 15 and 45 min residence time were conducted for five and nine times in each experiment. The most critical parameter to keep constant during the experiments was the desired residence time. The system had no feedback control resulting in that pH and redox potential were not adjusted during the experiments. This lead to varying pH and redox between the experiments. An overview of experiments performed at NTNU is shown in Table 4.1.

Table 4.1: Experimental parameters and results at NTNU.

Nr.	1	2	3	4
Temp. [°C]	65	65	65	65
Residence time [min]	45	45	45	15
Redox at filtration [mV]	467	428	225	400
pH at filtration	2.7	3.9	7.3	4.6
Fe_{total} [mg/L]	43.59	1.704	1.149	0.832
Fe^{3+} [mg/L]	43.59	1.704	1.070	0.832
Fe^{2+} [mg/L]	0.003	0.000	0.079	0.000
S	8	10	11	11
Cake resistance [m/kg]	$2.48 \cdot 10^{12}$	$6.84 \cdot 10^{10}$	$1.85 \cdot 10^{12}$	$1.76 \cdot 10^{12}$
Type precipitate	Ferrihydrite	Ferrihydrite	Ferrihydrite/Hematite	Ferrihydrite

Nr.	5	6	7	7.2
Temp. [°C]	29	29	79	90
Residence time [min]	15	15	15	Batch in 18.5 hours after experiment 7
Redox at filtration [mV]	-60	355	460	-
pH at filtration	6.4	5.4	3.2	-
Fe_{total} [mg/L]	1166	1.387	4.081	-
Fe^{3+} [mg/L]	26.66	0.832	4.002	-
Fe^{2+} [mg/L]	1139	0.555	0.079	-
S	2	3	16	-
Cake resistance [m/kg]	$2.39 \cdot 10^{13}$	$1.59 \cdot 10^{12}$	$3.53 \cdot 10^{11}$	$5.14 \cdot 10^{12}$
Type precipitate	Magnetite	Ferrihydrite	Ferrihydrite	Hematite

The temperature was regulated using water circulation resulting in a steady temperature with little or no variations as shown in Figure 4.1 and Figure 4.2, except for the experiment performed at 79°C. This was because of the water bath was set to maximum temperature so water had to be added regularly to keep the water level over minimum. For experiment 4 it can be seen a small drop in temperature at 1.5 hours. This may be caused by replenishment of water into the water bath with a subsequent reheating. This small temperature variation was assumed to not have an impact on the reaction.

Figure 4.1: Plot of temperature for the experiments with 45 min residence time performed at NTNU.
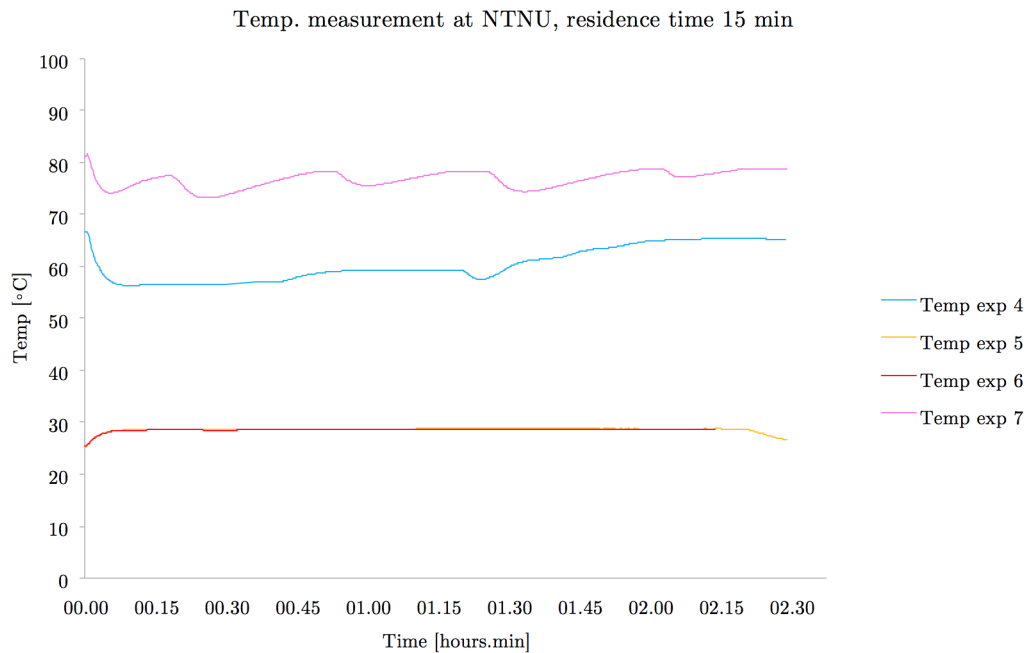
Figure 4.2: Plot of temperature for the experiments with 15 min residence time performed at NTNU.

From Figure 4.3 and Figure 4.6 it can be seen that after some adjustments at the beginning to reach desired values the pH and redox had small variations through each experiment. For experiment 3 in Figure 4.3 and Figure 4.5, 65°C and 45 min residence time, a decrease of 1 in pH and an increase in redox of 70 mV were observed lasting in a few minutes. This was due to the fact that the H_2O_2 container was moved a little and could indicate that the solution was not well mixed. However, the fact that the pH quickly reached the originaly stead state value and the solutions were stirred for 15-20 min, rather shows that just small adjustments in the pumps/system result in altering conditions.
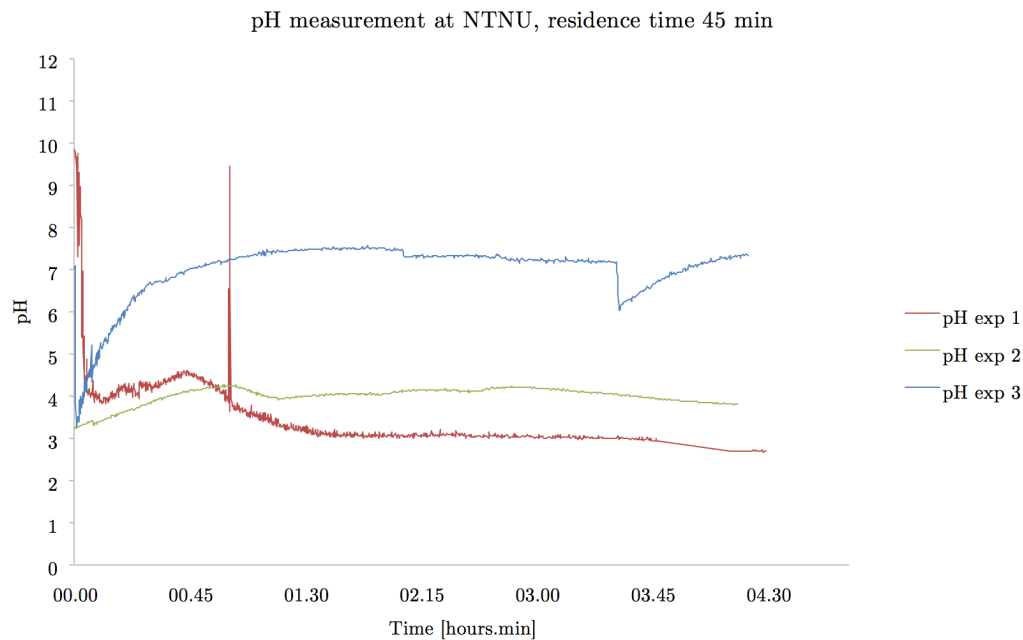
Figure 4.3: Plot of pH for the experiments with 45 min residence time performed at NTNU.

For experiment 5 in Figure 4.4 and Figure 4.6, 29°C and 15 min residence time, it can be seen a clear drop followed by an increase in pH and the opposite in redox. This was due to failure in the H_2O_2 pump before the end of the experiment. This resulted in obtaining magnetite based on the black color of suspension and further confirmed by the XRD-spectra as shown in Figure B.5, Appendix B. This shows the short amount of time without oxidation of divalent iron which is sufficient to obtain magnetite instead of trivalent iron precipitate.
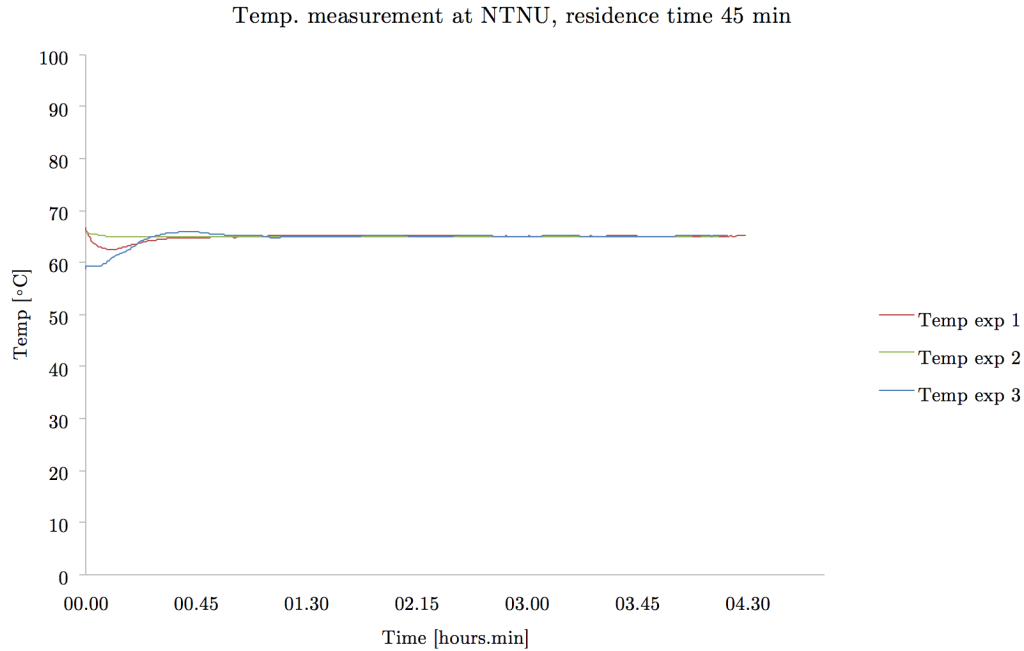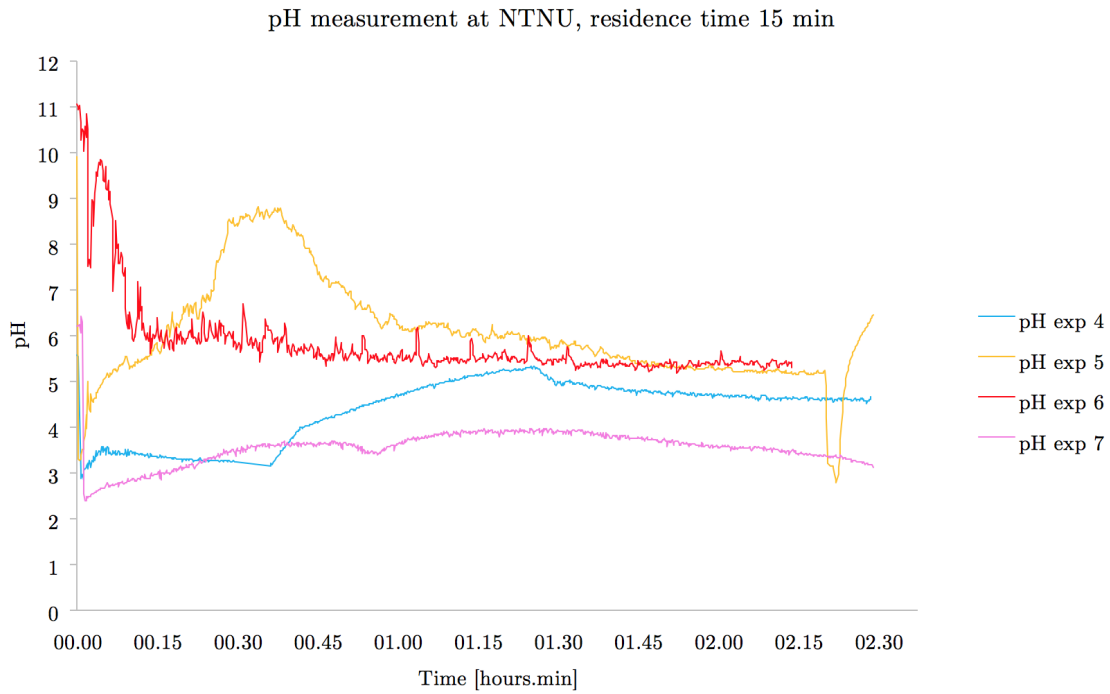
Figure 4.4: Plot of pH for the experiments with 15 min residence time performed at NTNU.
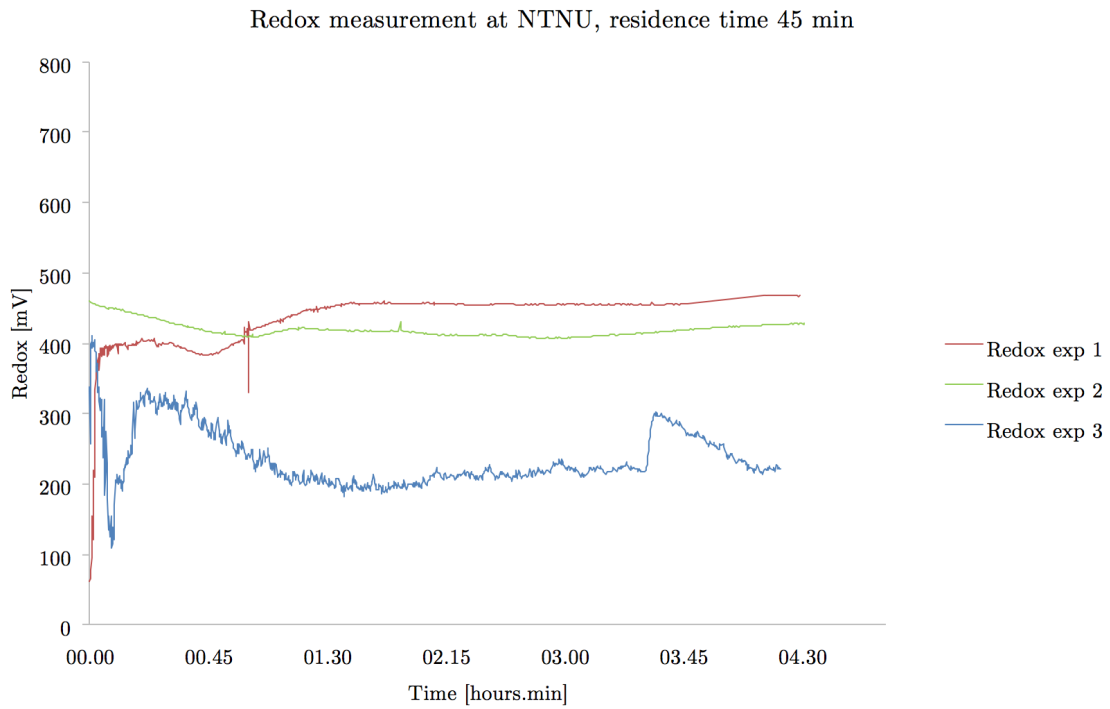
Figure 4.5: Plot of redox for the experiments with 45 min residence time performed at NTNU.

Redox measurement at NTNU, residence time 15 min
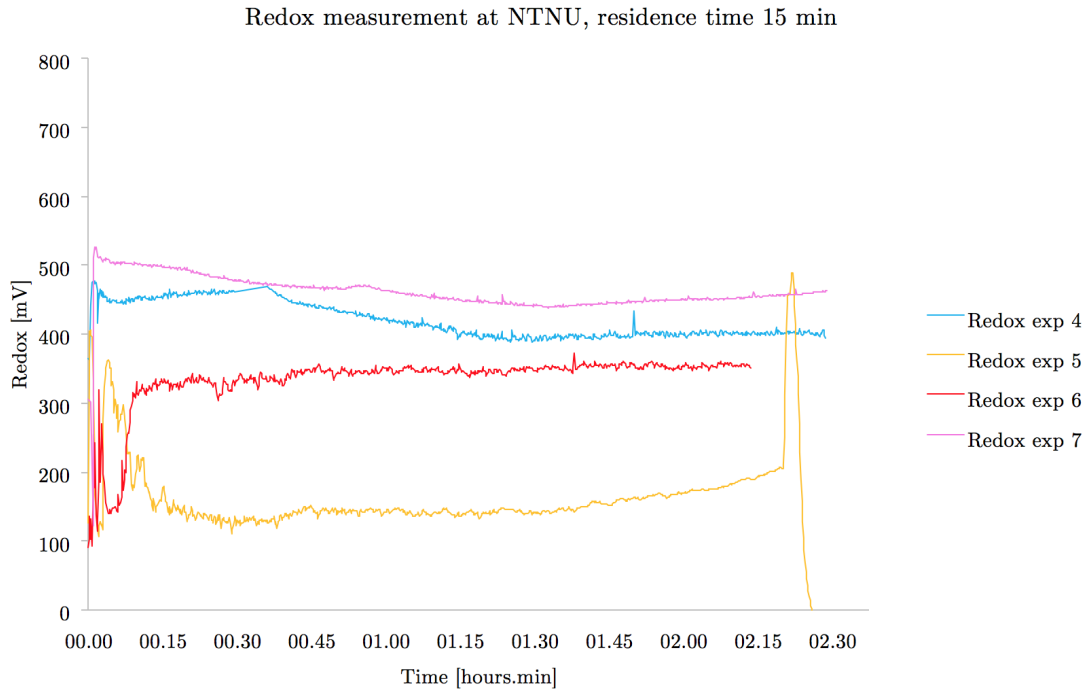
Figure 4.6: Plot of redox for the experiments with 15 min residence time performed at NTNU.

A difference in pH between the experiments was observed, despite using NaOH with the same concentration (0.35 M). This difference is thought to be caused by variations in the pump system. To confirm this, two calibration tests of the pumps were performed. Figure 4.7 confirms some variations of the pump performance. This can be the reason of difficulties having the same pH and redox for each experiment. The variation in pH was confirmed by experiment 1-3, using the same temperature, initial concentrations and residence time. In order to achieve more stable operating conditions the solution to the problem is to regulate the flow rate of the pumps manually at the beginning and/or during each experiment. An automatic feedback control system could also be used. Then it could be possible to maintain the same pH and redox, resulting in a better comparison of temperature and residence time.
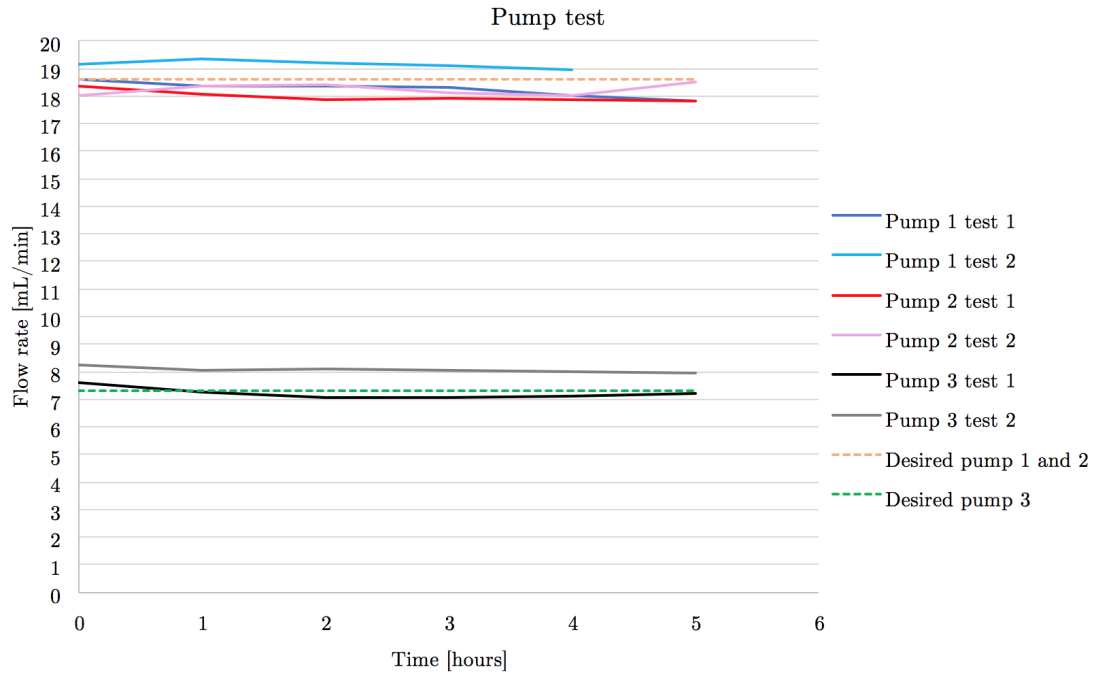
Figure 4.7: Plot of calibration tests performed for the pumps used at NTNU.

Alpha-tests to examine the filterability of the experiments were performed and from Figure 4.8 it could not be seen any clear correlation between the filterability, temperature and residence time. The standard deviation in Figure 4.8 and Figure 4.9 was calculated based on five filtration experiments using the same suspension filtrated at the same conditions. Calculations are attached in Appendix E, giving a standard deviation of 6.9%. This is a relatively low value so the results presented from the filtration tests are representative.

Filtration test for experiments performed at NTNU
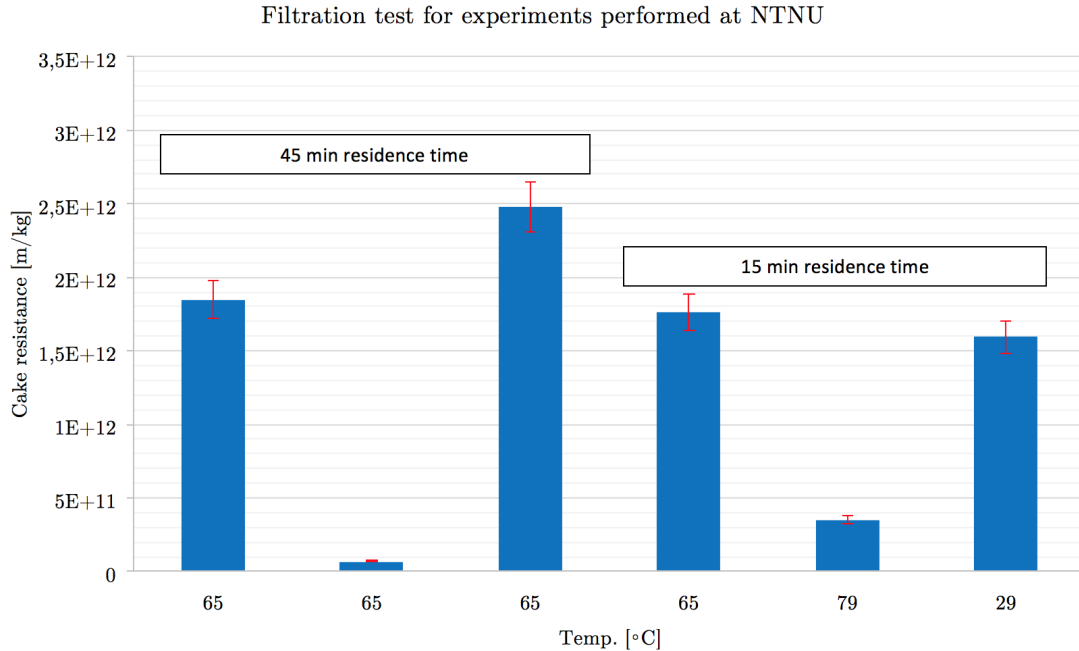
Figure 4.8:   Cake resistance plotted against temperature and residence time for the experiments performed at NTNU.

Figure 4.9 includes experiment 5 and 7.2, which clearly reveal that magnetite and hematite both have poorer filterability than ferrihydrite. This was regardless of temperature and residence time of the other experiments. This was further supported by the theory of filterability presented in section 2.5.2. It clearly states that particles with a spherical shape, like ferrihydrite, is expected to give a better filtration than other structures, such as magnetite (cubic/octahedral) and hematite (trigonal/hexagonal). The reason why spherical particles provide a better filterability may be because when the particles are packed together in a filter paper there are still space between the particles for filtrate to escape through.

For particles with clear edges in the crystal lattice like cubic and trigonal, there is a possibility for a very dense stacking during filtration, resulting in a lower filterability. From the SEM image of experiment 5 in Figure C.1 in Appendix C, it can be seen some cubic or octahedral alike structures that may confirm the structure of magnetite. The red squares drawn on the image may indicate areas of magnetite formation and the green squares may indicate that there was still some ferrihydrite remaining in the suspension, due to the fact that the transformation to magnetite did happen at the very end of the experiment due to pump error. There is only a few particles shown in the image, so no strong conclusions of the structure can be drawn.
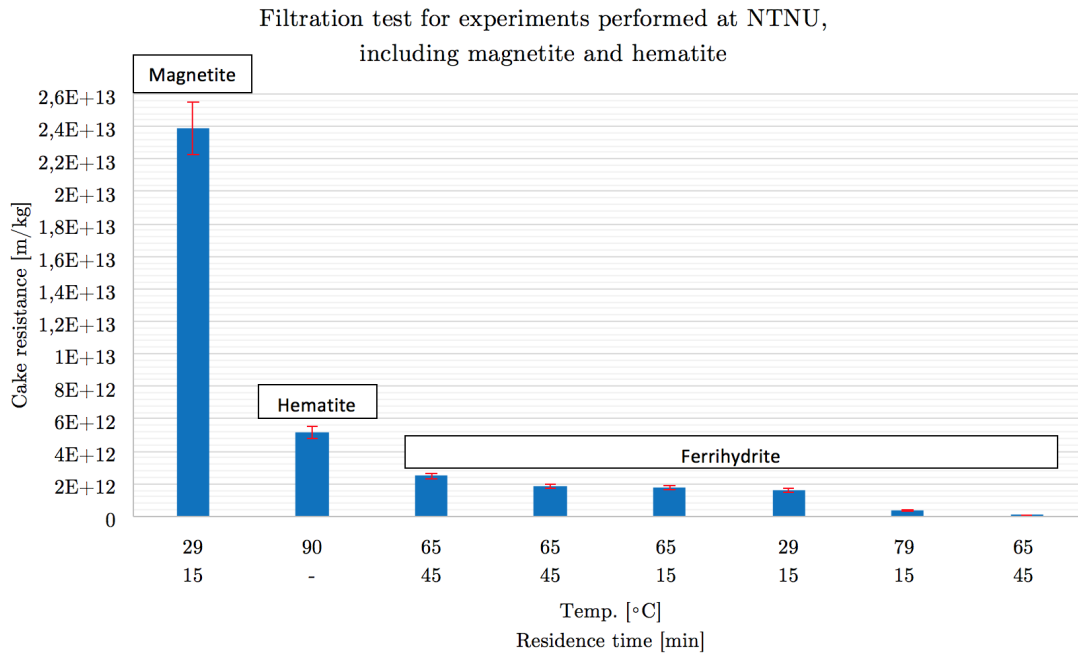
Figure 4.9: Cake resistance plotted against temperature and residence time for the experiments performed at NTNU, showing magnetite, hematite and ferrihydrite.

In Figure C.2 an example of ferrihydrite is shown for experiment 7 at 79°C with 15 min residence time, where the spherical particles may confirm ferrihydrite and bulk particles are marked in the red squares. Both of these two SEM images could together with Figure 4.9 confirm that spherical particles have a better filterability than cubic/octahedral particles. The fact that Figure C.2 shows large bulk particles of small ferrihydrite particles is in agreement with the theory presented in section 2.5.

25

Beside experiment 5 and 7.2 all of the experiments have confirmed ferrihydrite from the XRD-specters in Appendix B. The figures show the characteristic broad banded pattern for ferrihydrite, mentioned in section 2.5.1. However, experiment 3 in Figure B.3 somehow relatively strongly indicates hematite rather than ferrihydrite. This was not expected based on the theory presented in section 2.5, where it is stated that temperatures above 90°C are in general necessary to obtain hematite. However, it could be assumed that the chloride concentration in the system at NTNU was at a sufficient low value to produce hematite.

The initial chloride concentration for all the experiments at NTNU based in the addition of $FeCl_2$, was 0.36 M. This was higher than the assumed maximum value of 0.02 M for good conditions to produce hematite, as mentioned in section 2.5. More experiments have to be done to be able to confirm that hematite was produced. At this point the precipitate was more likely to consist of ferrihydrite than hematite, due to the chloride concentration and low temperature.

However, only considering the temperature of 90°C in 18.5 hours for experiment 7.2, hematite formation could be expected. Also for this experiment it was the same chloride condition as mentioned but this could indicate that elevated temperatures is more important than chloride concentration lower than 0.02 M. For experiment 7.2 it was not taken samples during the 18.5 hours of exposure time, therefore it is not known how long reaction time which is necessary to produce hematite.

The fact that formation of ferrihydrite was dominating the experiments at NTNU could be due to the use of hydrogen peroxide as an oxidation agent. In section 2.5.1 it is mentioned that the occurrence of ferrihydrite often is limited to a rapid oxidation of Fe^{2+}. This could indicate that using hydrogen peroxide gives a more rapid oxidation of divalent iron compared to for instance chlorine gas.

Before the stay at Glencore an experiment at the same initial conditions as for the presented experiments was performed, at 25°C with pH 2.6 where the residence time of 45 min was carried out 7 times, producing akaganeite based on Figure B.9 in Appendix B. This could indicate that the experiments at NTNU had to have more than 5 residence times to produce akaganeite with using residence time at 45 min. This despite the fact that the experiments with 9 residence times of 15 min not could obtain akaganeite. Time limitations were the reason why the rest of the experiments with 45 min residence time could not be ran more than 5 times.

Before the experiments at NTNU were performed it was expected that higher temperatures would give a more effective filtration based on the alfa test. It was also assumed that longer residence time would contribute to a better filterability of the suspension. Based on Equation 4 in section 2.2, a lower ionic activity of iron ions would give a lower supersaturation, achieved with a longer residence time. Then a lower concentration of free iron ions could be obtained because of the longer reaction time and the ability of iron ions to become iron oxides/hydroxides. If a lower supersaturation could be obtained it could result in a lower nucleation rate based on Equation 5 and Equation 6 in section 2.3.

Equation 4 also shows the supersaturations high dependence of pH based on the activity of hydroxide raised in third. This was confirmed by Figure 4.10 for experiments performed at 65°C with 45 and 15 min residence time. There can be seen that the supersaturation was decreasing with decreasing pH, which surpasses the effect of varying the residence time between 15 and 45 min. In experiment 1-3, performed with 45 min residence time, it can be seen from Table 4.1 that the supersaturation actually also are increasing along with decreasing trivalent iron concentration. This could also confirm that the pH was the major parameter for supersaturation due to the fact that the activity of OH^- was raised in third.
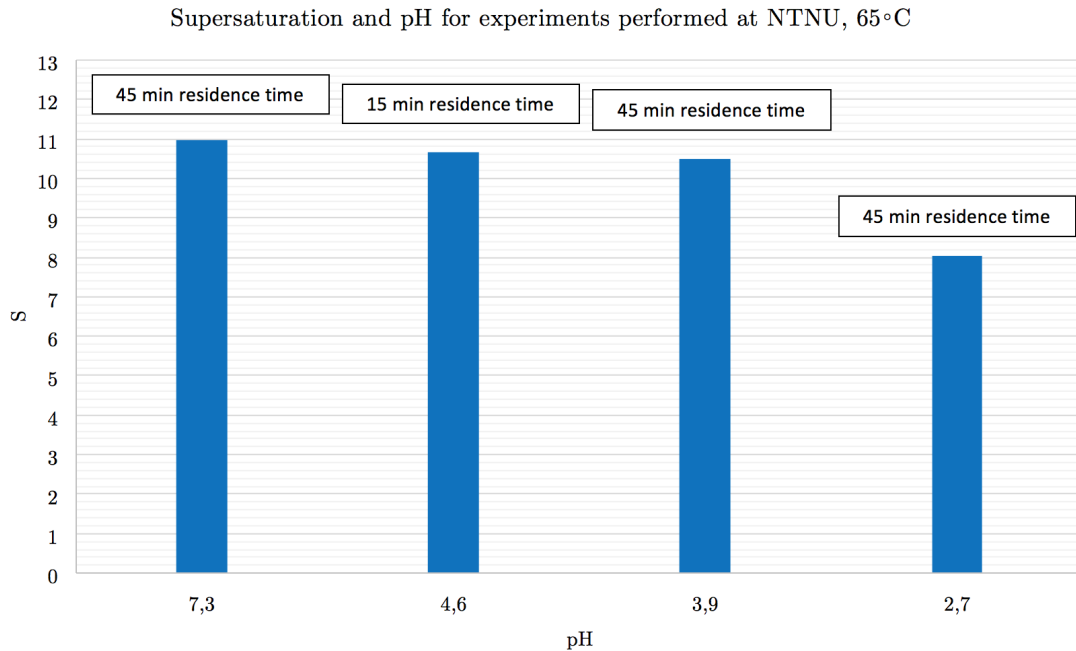
Figure 4.10: Supersaturation plotted against pH for the experiments performed at NTNU.

Based on this there was tried to find a connection between filterability and pH instead of temperature and residence time. From Figure 4.11 for experiments performed with 45 min residence time at 65°C it can be seen that there was no clear connection between pH and the filterability of the suspension. This independence between filterability and pH made it desirable to have a closer look at the temperature part of Equation 5 and Equation 6.

The mentioned equations show an importance of temperature to the nucleation rate, where a higher temperature could result in a higher nucleation rate. Further, a higher rate of nucleation could produce high amount of small particles instead of having the opportunity to let the nucleated particles grow large. Figure 4.8 shows no signs of temperature dependency to the filtrated particles. If the supersaturation is considered a higher supersaturation would also give a higher nucleation rate. From experiment 1, 2, 4, 6 and 7 from Table 4.1, resulting in ferrihydrite, it could not be confirmed that higher supersaturation would result in a poorer filtration due to higher nucleation rate.

Filtration test for experiments performed at NTNU, 65°C with 45 min residence time
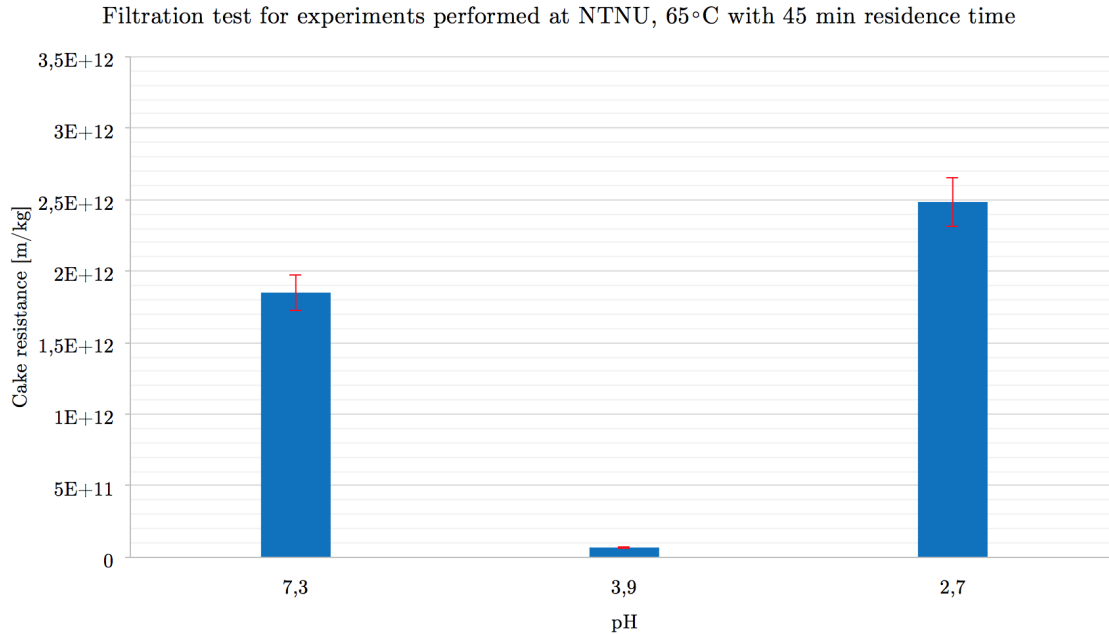
Figure 4.11: Cake resistance plotted against pH for the experiments performed at NTNU.

This confirms that it is very difficult to compare experiments where all of the parameters are varying. The experimental work do confirm some theoretical connections between supersaturation, pH and iron ion activity. It was assumed that all of these varying parameters do contribute to the filterability in different degrees. To be able to see the clear picture of which parameters that are the most important to increase the filterability, the parameters have to be isolated in a systematic way. This could be done by, as mentioned, feedback control of pH and redox.

4.2   Experiments at Glencore

During a three week stay at Glencore experiments with solution from the process used as feed material, were performed to see how temperature and residence time had an impact on the filterability of the iron oxide/hydroxide precipitate. All of the experiments with process solution were performed using the same pH and redox potential. This were to be able to compare the experiments based on temperature and residence time. As shown from the experiments performed at NTNU, it was necessary to maintain pH and redox constant between the experiments to be able to produce the same type of precipitate and make the experiments comparable.

An overview of experiments performed at Glencore is shown in Table 4.2. Some of the samples were analyzed with XRD at Elkem, Figure 4.14, Figure D.1, Figure D.2 and Figure D.3. These XRD-specters begin at a higher intensity than for the samples analyzed at NTNU, due to use of another XRD apparatus. The specters are compared based on the intensity and pattern of the peaks causing no negative effect on the comparison.

Experiment 1-3 were performed using the same process solution, where a new process solution was collected for experiment 4 and 5, this was due to storage limitations. The iron content was approximately the same in the feed material, so it is assumed that the amount of iron fed to the reactor was equal for each experiment.

Table 4.2: Experimental parameters and results at Glencore.

Nr.	1	2	3	4	5	Test
Temp. [°C]	65	30	90	65	65	65
Residence time [min]	75	75	75	45	75	45
Redox at filtration [mV]	480	480	480	480	480	138
pH at filtration	1.8	1.8	1.8	1.8	1.8	2.5
Fe_{total} [mg/L]	Not measured	232	620	718	482	Not measured
Fe^{3+} [mg/L]	Not measured	132	418	448	348	Not measured
Fe^{2+} [mg/L]	Not measured	100	202	270	134	Not measured
Cl^- [mg/L]	Not measured	318800	319200	305200	315200	Not measured
Process solution	1	1	1	2	2	-
S	-	2	23	10	10	-
Cake resistance [m/kg]	$1.28 \cdot 10^{12}$	$1.39 \cdot 10^{12}$	$1.19 \cdot 10^{11}$	$3.25 \cdot 10^{12}$	$1.20 \cdot 10^{12}$	Not measured
Type precipitate	Akaganeite	Akaganeite	Akaganeite	Akaganeite	Akaganeite	Akaganeite

The temperature, pH and redox potential had feedback control using signals from the pH og redox electrodes sent to a computer program. This made it possible to maintain the same pH and redox for each experiment. The temperature was regulated using a heat cap under the reactor resulting in some small oscillations of 2-3°C, except for the experiment performed at 30°C. This may be caused by the fact that heating was unnecessary almost through the whole experiment due to the low temperature. From Figure 4.12 and Figure 4.13 it can be seen that after some adjustments at the beginning to reach desired values, the pH and temperature were constant through each experiment.
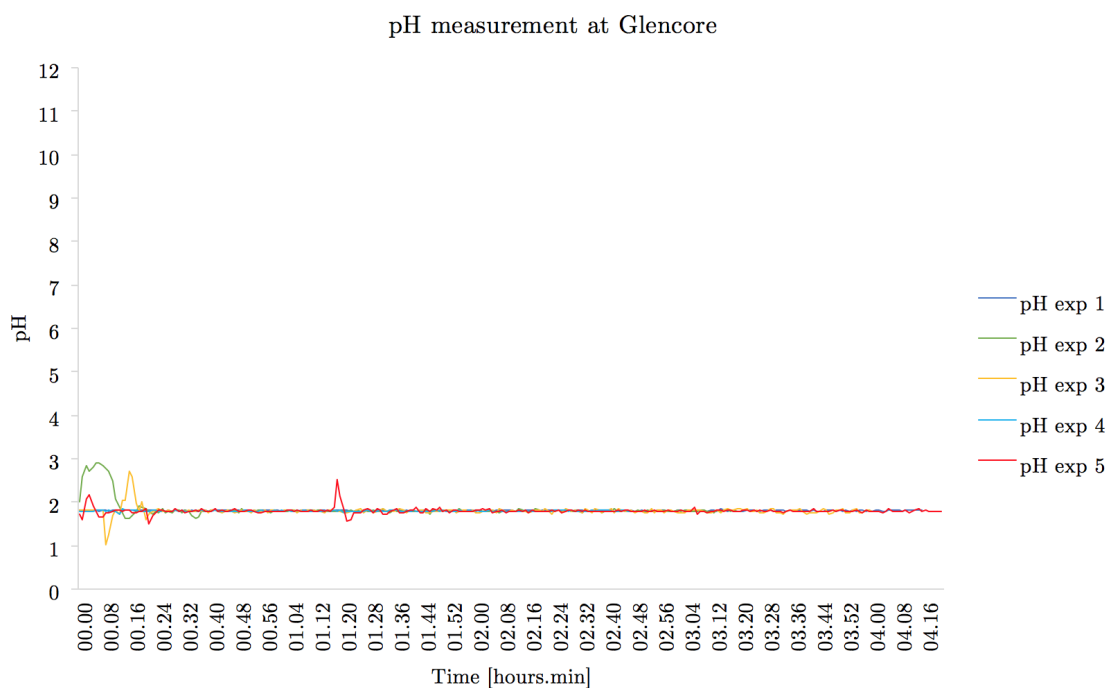

Figure 4.12: Plot of pH through each experiment performed at Glencore.
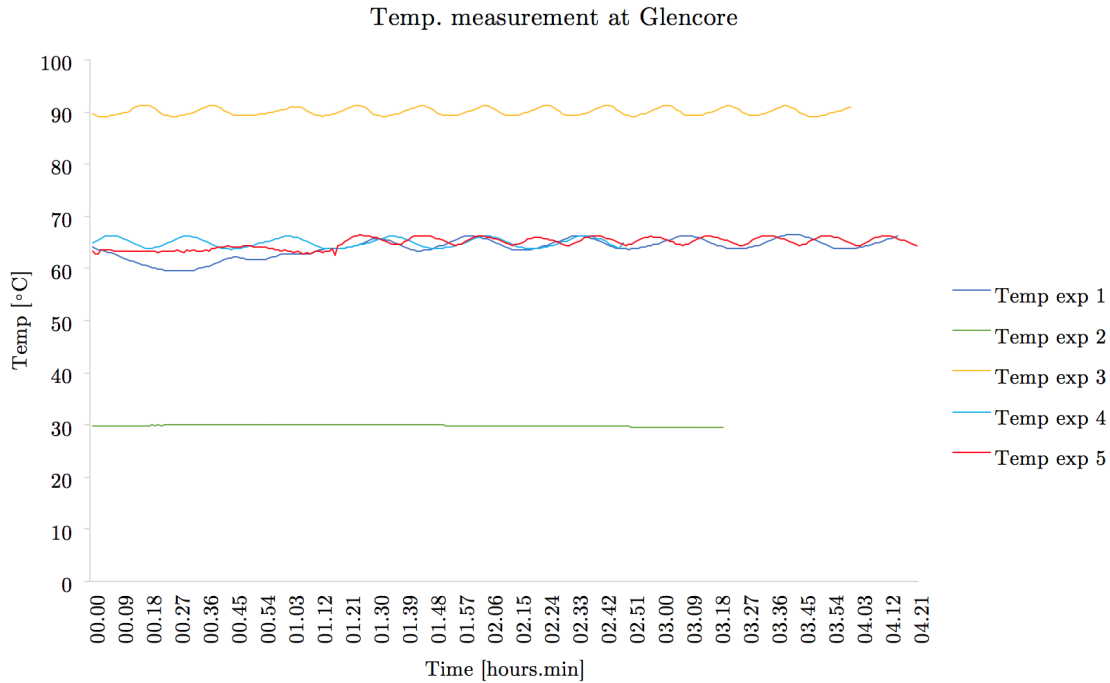
Figure 4.13: Plot of temperature through each experiment performed at Glencore.

All of the experiments performed at Glencore with the process solution as feed material produced akaganeite, shown in Appendix D by XRD-analysis. This favoring of akaganeite at the experimental conditions could be expected based on the theory presented in section 2.5. It is stated that in high chloride concentrations at low pH and elevated temperature (e.g. 60°C) akaganeite formation is favored. The experiments were performed at 30, 65 and 90°C with pH 1.8 and chloride concentrations of the filtrates from the filtration tests in average at 315 g/L. The experiment performed at 30°C produced akaganeite which could indicate that high chloride concentration and/or low pH is more important for the formation og akaganeite than elevated temperatures.

An experiment using divalent iron chloride instead of process solution as feed material, sodium hydroxide as a base instead of nickel carbonate and hydrogen peroxide as an oxidant instead of chlorine gas, was performed at Glencore. This in order to examine if akaganeite could be produced without high concentrations of chloride. The XRD-spectra in Figure 4.14 indicates that akaganeite was produced. The pH for this experiment was also relatively low (pH 2.5) at 65°C, so this might indicate that low pH are determining for producing akaganeite to a greater extent than the amount of chloride.
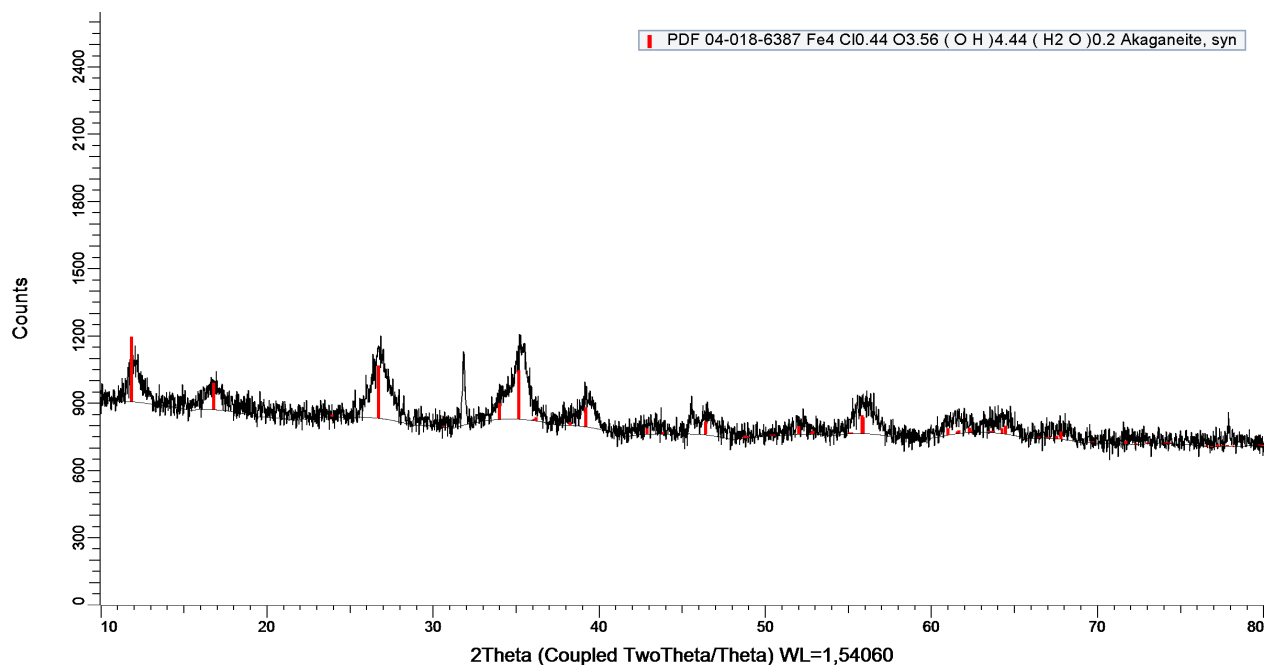

Figure 4.14: XRD-spectra from experiment at Glencore using divalent iron chloride, sodium hydroxide and hydrogen peroxide, at 65°C with 45 min residence time, indicating akaganeite. Analyzed at Elkem.

A sample obtained directly from the process at Glencore was analyzed with XRD. The XRD-spectra in Figure 4.15 indicated that akaganeite also was precipitated in the industrial process at Glencore, where the process is carried out at the same pH and redox as for the experiments and at 65°C. When comparing the XRD-spectra with experiment 4 in Figure D.4 in Appendix D, obtained at the same conditions and residence time as for the process, the intensity of the peaks was approximately the same for the two samples. This could indicate that akaganeite obtained in the process and in the laboratory possess the same crystallinity, which may give the same filterability. This could be tested by filtrating a sample solution

from the process.

A SEM image of the process sample is shown in Figure 4.16. The sample was washed and dried before sample preparation. It was difficult to assess the shape of these particles but the picture may indicate that tetragonal akaganeite particles were obtained. The spherical particles which can be seen may be some residue that have not been washed out from the sample or it could be spherical ferrihydrite bulk particles not yet transformed into akaganeite.
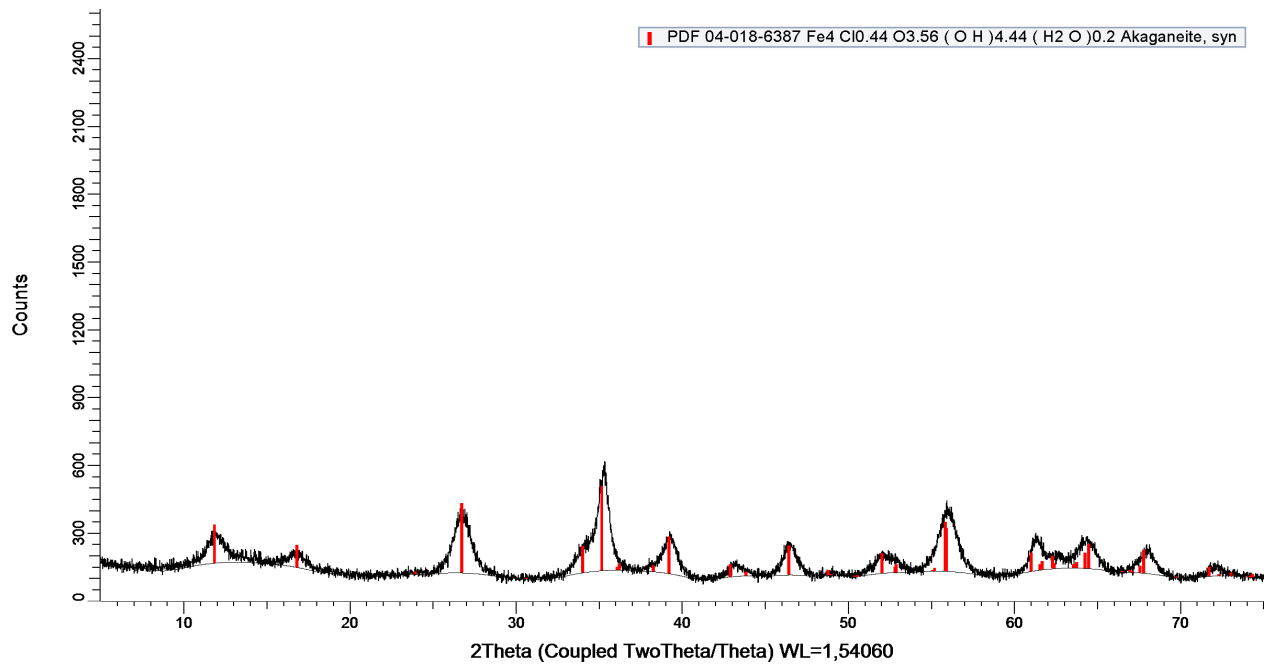

Figure 4.15: XRD-spectra of a sample obtained directly from the process at Glencore indicating akaganeite.

Figure 4.16: SEM image of a sample obtained directly from the process at Glencore. The background is fibers from the filter paper.

Alpha-tests to examine the filterability of the experiments were performed and Figure 4.17 clearly indicates that the filterability increases with higher temperature. It can also be seen that longer residence time gives a better filtration and in fact have a higher impact on the filterability than the temperature.

All of the experiments were performed at the same pH, redox and iron content in the feed material and from Equation 4 in section 2.2 it can be seen that since the pH was constant between the experiments, the iron activity may be the determining parameter for the supersaturation. Based on this the supersaturation could be expected to be lower for longer residence time due to lower concentration of trivalent iron ions in the suspension. This is because of the iron ions have longer reaction time in the reactor before exiting and thus longer time to form iron oxide/hydroxide. Therefore, lower supersaturation is desired at Glencore to be able to remove most of the iron as an impurity in the process. From Table 4.2 it can be seen that experiment 4 and 5 at 65°C with 45 and 75 min residence time, had the same supersaturation but longer residence time gave better filterability. To confirm the fact that the supersaturation was the same at different residence time, more experiments have to be performed.

Based on this the explanation for better filterability with longer residence time might be in the chloride content, where experiment 5 with 75 min residence time contained 10 g/L more chloride than experiment 4 at 45 min residence time. This might indicate that the conditions for akaganeite formation were better for the experiment with longer residence time. To draw a stronger conclusion more experiments on residence time have to be done.

As mentioned for the NTNU results, if Equation 5 and Equation 6 in section 2.3 are considered, it is clear that the nucleation rate for a homogeneous nucleation is dependent on temperature and supersaturation. Both higher supersaturation and higher temperature could result in a higher nucleation rate.

If the experiments is connected to this, conditions at 90°C will have higher nucleation rate than at 30°C and 65°C. This is expected to give a poorer filterability due to nucleation of new particles instead of let the particles grow larger. If the supersaturation is considered, it was a lower value of supersaturation for the experiment at 30°C compared to the one at 90°C. From Table 4.2 it can be seen that higher temperature give better filtration, despite that this together with high supersaturation would give higher nucleation rate. Because the pH was the same for all the experiments the initial hydroxide concentration is the same. The increase of supersaturation with higher temperatures is therefore explained by the increasing activity of hydroxide, calculated using the Visual MINTEQ computer program, shown in Figure 4.18.
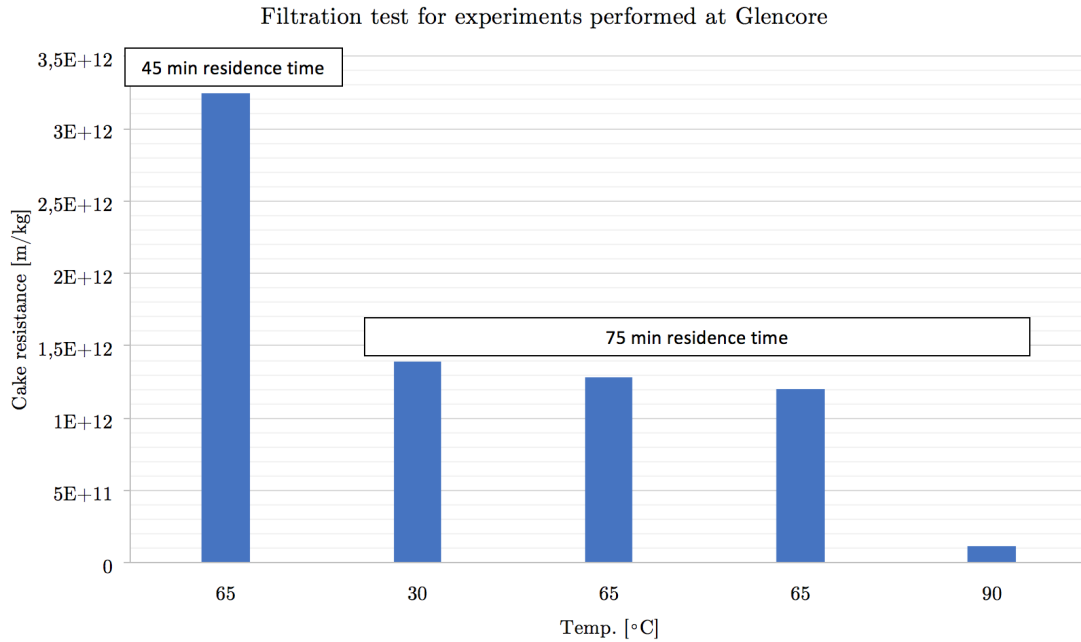
Figure 4.17:   Cake resistance plotted against temperature and residence time for the experiments performed at Glencore using process solution as feed material.
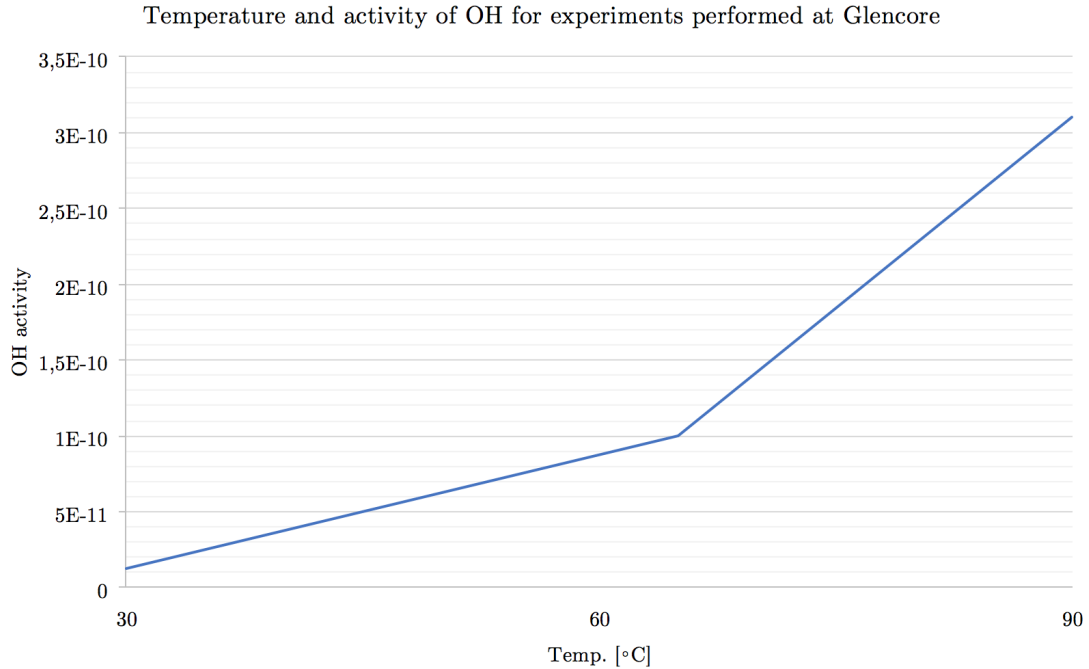

Figure 4.18:   The activity of hydroxide plotted against temperature for the experiments performed at Glencore, using process solution as feed material.

To confirm that the variations were small between parallel experiments at the same temperature, pH, redox and residence time, experiment 1 and 5 at 65°C with 75 min residence time were performed. The filterability from the alpha-test in Figure 4.17 shows that the variety between the experiments were small compared to higher temperature and shorter residence time. The difference between the parallells at 65°C with 75 min residence time was $8 \cdot 10^{10}$ and the difference between the experiments at 65°C with highest cake resistance and the one performed at 30°C was $11 \cdot 10^{10}$.

It could be argued that the difference between the parallels and the temperatures at 30°C and 65°C were too close to conclude that it would be beneficial to increasing the temperature from 30°C to 65°C. When the difference in the parallels was considered, 65°C had an alpha of $3 \cdot 10^{10}$ lower than 30°C which may be a large enough difference to claim that a process temperature of 30°C was not beneficial for the filtration process. As mentioned, the crystallization process at Glencore is currently performed at 65°C where increasing from 65°C to 90°C is of interest, which seems to be beneficial from this study.

When the XRD-results in Appendix D are compared it can be seen that the experiment resulting in the best filterability at 90°C have the highest intensity of the peaks. The largest difference in intensity is for 30 and 90°C with 75 min residence time in Figure D.2 and Figure D.3. Compared to the filterability, this could indicate that 90°C gives more crystalline precipitate than 30°C, which could be the reason for a more effective filtration. If Figure D.4 at 65°C with 45 min residence time and Figure D.1 and Figure D.5 at 65°C with 75 min residence time are compared, there is no clear correlation between the intensity of the peaks and filterability.

For the SEM images of the samples produced at Glencore, the images to the left hand side are used to analyze the average size of the particles. The pictures to the right hand side are used to show how an extract of particles look like with a higher magnification, and is not representative for the average particle size of the samples. The samples were washed and dried before sample preparation. When comparing the SEM images of iron precipitate produced for the experiments at 65°C, with 75 min residence time in Figure 4.19 and Figure 4.23 and 45 min residence time in Figure 4.22, it seems that longer residence time produce larger average particle size. This complies with the fact that longer residence time result in better filterability shown in Table 4.2.
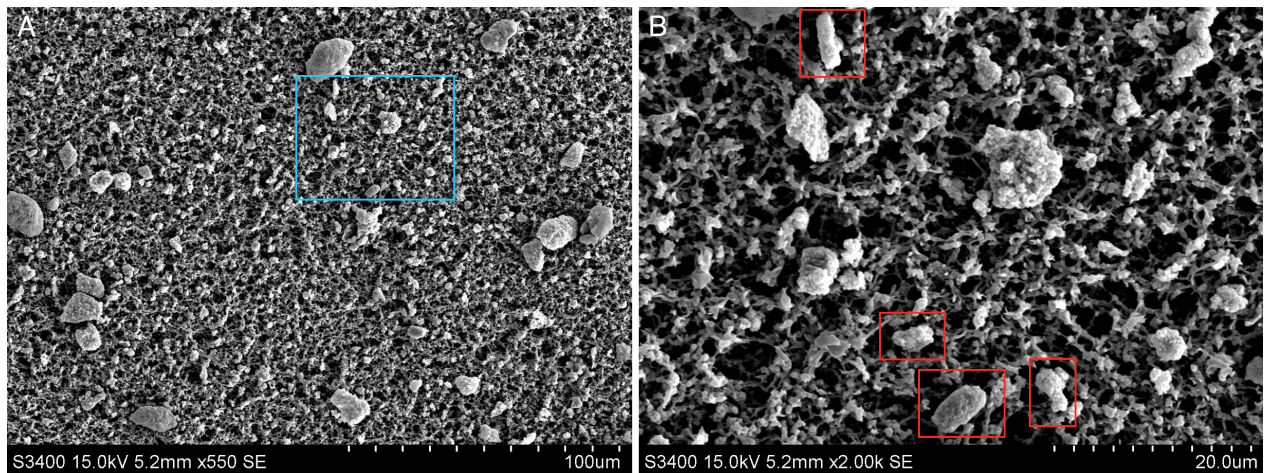

Figure 4.19: SEM images of experiment 1 performed at Glencore, 65°C with 75 min residence time. The blue square in A shows the area which is at a higher magnification in B.

From the SEM images of the experiments at 30 and 90°C with 75 min residence in Figure 4.20 and Figure 4.21, respectively, it can be seen that the average particle size increases with increasing temperature. If this is compared to the fact that the filterability was better for iron precipitate produced at higher temperature, this confirms that larger particles give better filtration shown in Table 4.2. The fact that larger particles are desired for an effective filtration is stated in section 2.5.2.
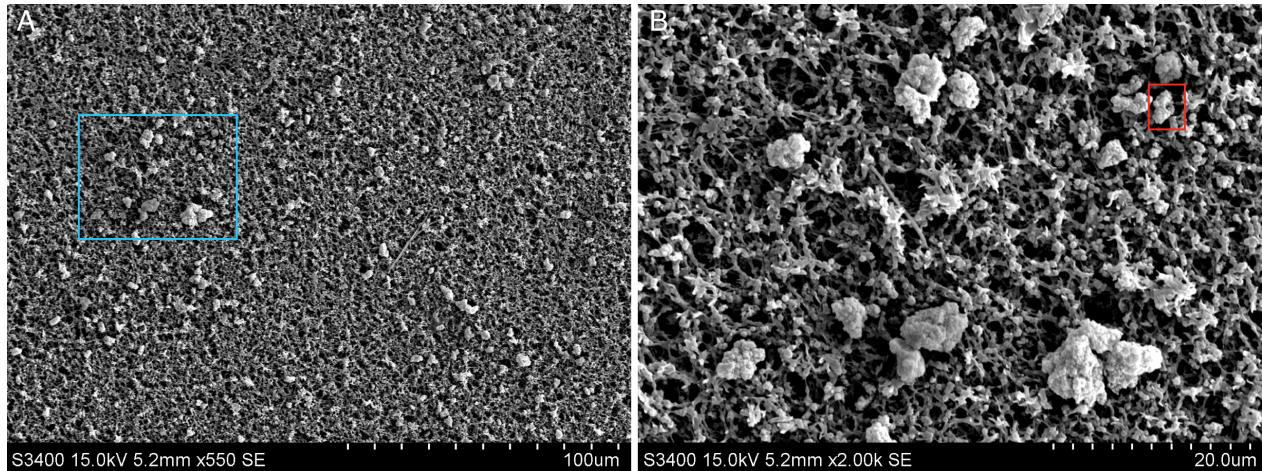

Figure 4.20: SEM images of experiment 2 performed at Glencore, 30°C with 75 min residence time. The blue square in A shows the area which is at a higher magnification in B.
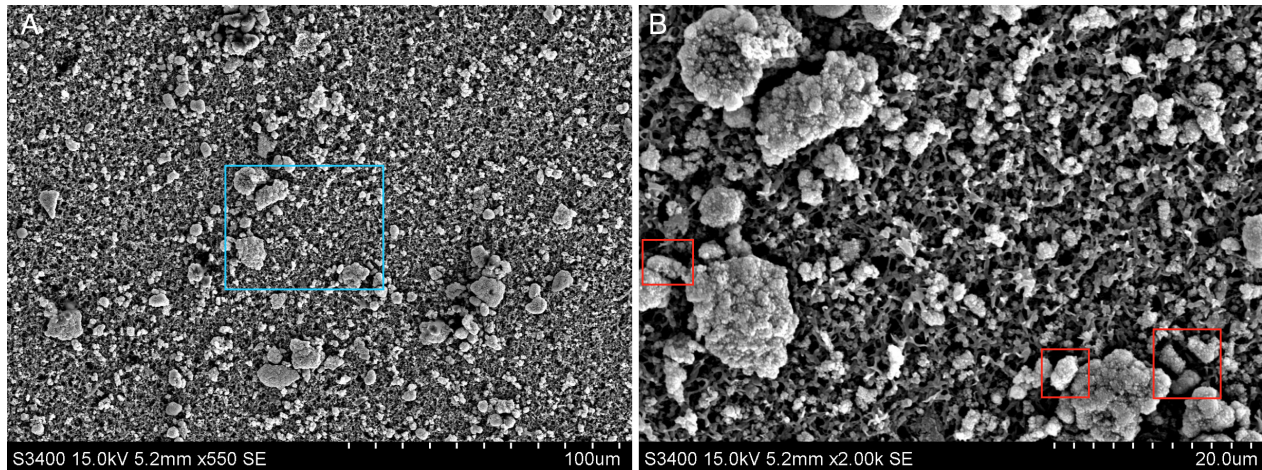

Figure 4.21: SEM images of experiment 3 performed at Glencore, 90°C with 75 min residence time. The blue square in A shows the area which is at a higher magnification in B.
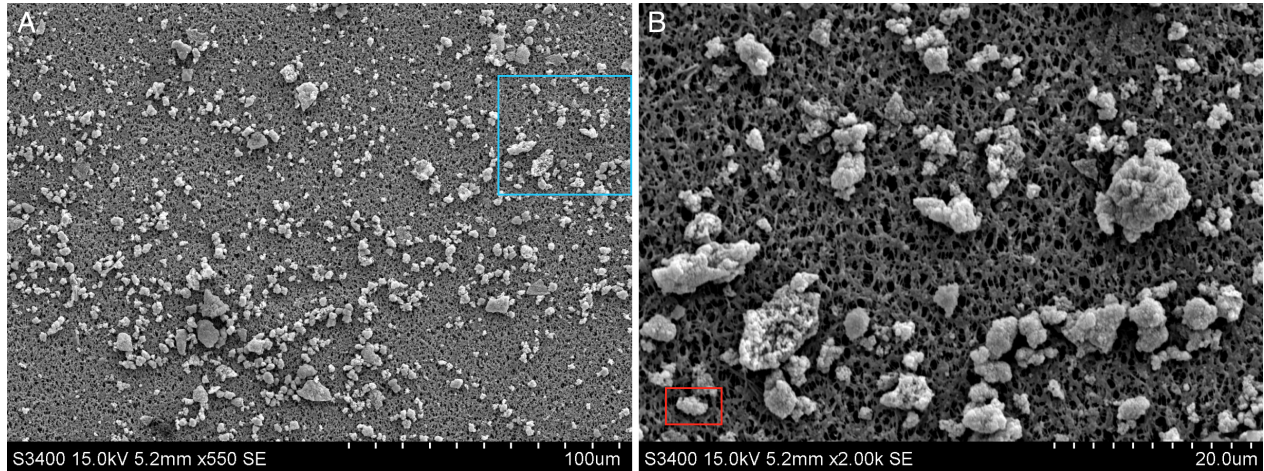
Figure 4.22: SEM images of experiment 4 performed at Glencore, 65°C with 45 min residence time. The blue square in A shows the area which is at a higher magnification in B.

From the parallel experiments performed at 65°C with 75 min residence time, Figure 4.19 and Figure 4.23 show that the average particle size for these two experiments seems to be relatively equal.
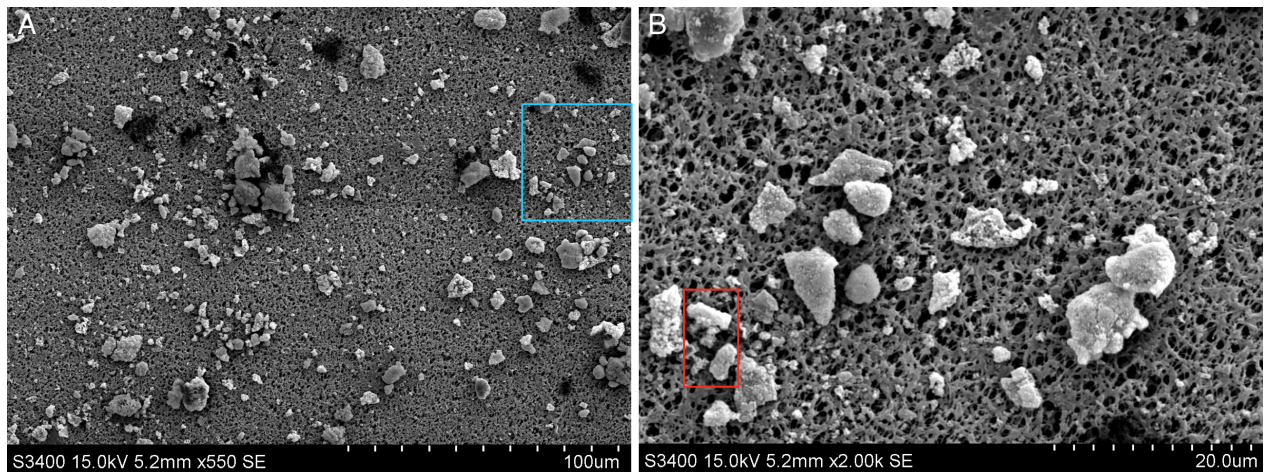

Figure 4.23: SEM images of experiment 5 performed at Glencore, 65°C with 75 min residence time. The blue square in A shows the area which is at a higher magnification in B.

From the SEM images in Figure 4.19 to Figure 4.23 it was difficult to conclude the shape of the particles. The red squares in the figures may indicate the tetragonal structure of akaganeite particles. The smallest spherical/trigonal alike particles and the bulk particles which they obtained, could indicate either very small akaganeite particles or ferrihydrite which not yet have been transformed into akaganeite.

5 Conclusions

The background for this thesis was crystallization of iron in nickel production at Glencore and a review of filterability properties of iron oxide/hydroxide precipitate. The aim of this thesis was to determine how different temperatures and supersaturation, due to residence time, affected the crystalline type and filterability of iron oxide/hydroxide precipitate.

At NTNU the precipitate was found to be ferrihydrite but a clear correlation between filterability, temperature and residence time could not be ascertained. Akaganeite was obtained for all the experiments at Glencore both for using process solution and divalent iron chloride as feed material. The filterability were improved both with increasing temperature and longer residence time, where the residence time had a higher impact than the temperature.

It was concluded that to be able to compare different temperatures and residence times the pH and redox potential have to be kept constant between each experiment. This could be done by using feedback control.

6   Further Work

The suggestion for further work is based on the work and results obtained during this thesis. To be able to compare the experiments using divalent iron chloride as feed material, pH and redox potential have to be kept constant between the experiments. Then it can be more easily determined whether it is possible to obtain akaganeite using divalent iron chloride, sodium hydroxide and hydrogen peroxide. It may also be clearer if the chloride concentration has a major impact when producing akaganeite.

If it is revealed that it is still difficult to produce akaganeite at controlled pH and redox conditions at varying temperatures and residence time, sodium chloride may be added to the suspension at the beginning or during the experiments. This could give a high enough chloride concentration to produce akaganeite. Since the experiments at Glencore and NTNU were performed using different oxidation agents, using chlorine gas to oxidize divalent iron chloride could indicate if the chlorine gas was the reason why akaganeite was more easily obtained at Glencore.

The test experiment performed at NTNU ran at 7 residence times of 45 min at 25°C, resulted in akaganeite. Based on this it could be valuable to examine the possibility to produce akaganeite when residence time of 45 min is ran for a longer time at different temperatures.

The suspension at NTNU kept at 90°C for 18.5 hours taken from the suspension obtained at 79°C, was determined to be hematite. Additionally, one experiment performed at 65°C may indicate hematite. Based on this it could be interesting to investigate which conditions that are necessary to obtain hematite and to determine if temperature, pH or the experiment time that have the highest impact.

Since the stay at Glencore was time limited more experiments with process solution as feed material is recommended to provide more information about the connection between temperature, residence time and filterability. Since it was difficult to produce akaganeite at NTNU with varying and periodically relatively high pH, it could be interesting to see how higher pH (4-6) would impact experiments using process solution at Glencore.

7 References

[1] Crundwell F. K., Moats M. S., Ramachandran V., Robinson T. G., and Davenport W. G. *Extractive Metallurgy of Nickel, Cobalt and Platinum-Group Metals*. Elsevier, 2011.

[2] Heskestad R. Krystallisasjon og faststoffseparasjon. betydningen av krystallisasjonsparametre på krystallstørrelsesfordeling, morfologi og filtreringsegenskaper. *Specialization project at NTNU*, 2008.

[3] Myerson A. *Handbook of Industrial Crystallization*. Butterworth-Heinemann, 2002.

[4] Schwertmann U. and Cornell R. M. *Iron Oxides in the Laboratory - Preparation and Characterization*. VCH, 1991.

[5] Streat M., Hellgardt K., and Newton N.L.R. Hydrous ferric oxide as an adsorbent in water treatment part 1. preparation and physical characterization. *Process safety and environmental protection*, 2008.

[6] Dotterud O. M., Peek E. M. L., Stenstad O., and Ramsdal P. O. *Iron Control and Tailings Disposal in the Xstrata Chlorine Leach Process*. 2009.

[7] Sedzik J. *Molecules : Nucleation, Aggregation and Crystallization*. World Scientific, 2009.

[8] Mullin J. W. *Crystallization*. Elsevier, 4. edition, 2001.

[9] Matthews J. A. *Encyclopedia of Environmental Change*. SAGE Publications, Ltd, 2014.

[10] Bralla J. G. *Handbook of Manufacturing Processes - How Products, Components and Materials are Made*. Industrial Press, 2007.

[11] Beckmann W. *Crystallization: Basic Concepts and Industrial Applications*. Wiley-VCH, 2013.

[12] Loana M., Parkinsona G., Newmanb M., and Farrowc J. Iron oxy-hydroxide crystallization in a hydrometallurgical residue. *Journal of Crystal Growth 235*, 2002.

[13] Schwertmann U. and Cornell R. M. *The Iron Oxides: Structure, properties, reactions, occurrence and uses.* VCH, 1996.

[14] Van Driessche A. E. S., Kellermeier M., Benning L. G., and Gebauer D., editors. *New Perspectives on Mineral Nucleation and Growth.* Springer International Publishing, 2017.

[15] Ståhl K., Nielsen K., Jiang J., Lebech B., Hanson J. C., Norby P., and van Lanschot J. On the akaganeite crystal structure, phase transformations and possible role in post-excavational corrosion of iron artifacts. *Corrosion Science*, 2003.

[16] Peterson K. M. *Nucleation, growth, and phase transformation mechanisms of the iron (oxy)hydroxides.* PhD thesis, The Pennsylvania State University, 2015.

[17] Lee S. A., Fane A. G., Amal R., and Waite T. D. *The effect of floc size and structure on specific cake resistance and compressibility in dead-end microfiltration.* Separation Science and Technology, 2003.

[18] Svarovsky L. *Characterization of particles suspended in liquids, In: Solid- Liquid Separation.* Butterworth-Heinemann, 1981.

[19] Hwang K. J., Wu Y. S., and Lu W. M. *The surface structure of cake formed by uniform-sized rigid spheroids in cake filtration.* Powder Technol, 1996.

[20] Wakeman R. *The influence of particle properties on filtration.* Elsevier, 2007.

[21] Ripperger S., Gösele W., and Alt C. *Filtration, 1. Fundamentals.* Ullmann's Encyclopedia of Industrial Chemistry, 2009.

[22] Cheremisinoff N. P. *Liquid Filtration.* Elsevier, 2nd. edition, 1998.

[23] Wakeman R. J. and Tarleton E. S. *Filtration.* Elsevier, 1. edition, 1999.

[24] Ladislav S. *Solid-Liquid Separation.* Elsevier Science, 4th edition, 2000.

[25] Kestin J., Khalifa H. E., and Correia R. J. Tables of the dynamic and kinematic viscosity of aqueous nacl solutions in the temperature range 20-150c and the pressure range 0.1-35 mpa. *J. Phys. Chem. Ref. Data. Vol. 10. No. 1*, 1981.

A   Physical Data for the Relevant Chemicals

Table A.1: Physical data for the chemicals used for this thesis.

Chemical	Producer	Mole Weight [g/mole]	Assay [%]	CAS
Iron (II) chloride tetrahydrate	VWR Chemicals	198.81	Min. 99.0	13478-10-9
Hydrogen peroxide	VWR Chemicals	34.01	30.6	7722-84-1
Sodium hydroxide	VWR Chemicals	40.00	99.3	1310-73-2
Nickel carbonate	Glencore process solution	-	-	-
Feed material	Glencore process solution	-	-	-

B XRD-specters from Experiments Performed at NTNU
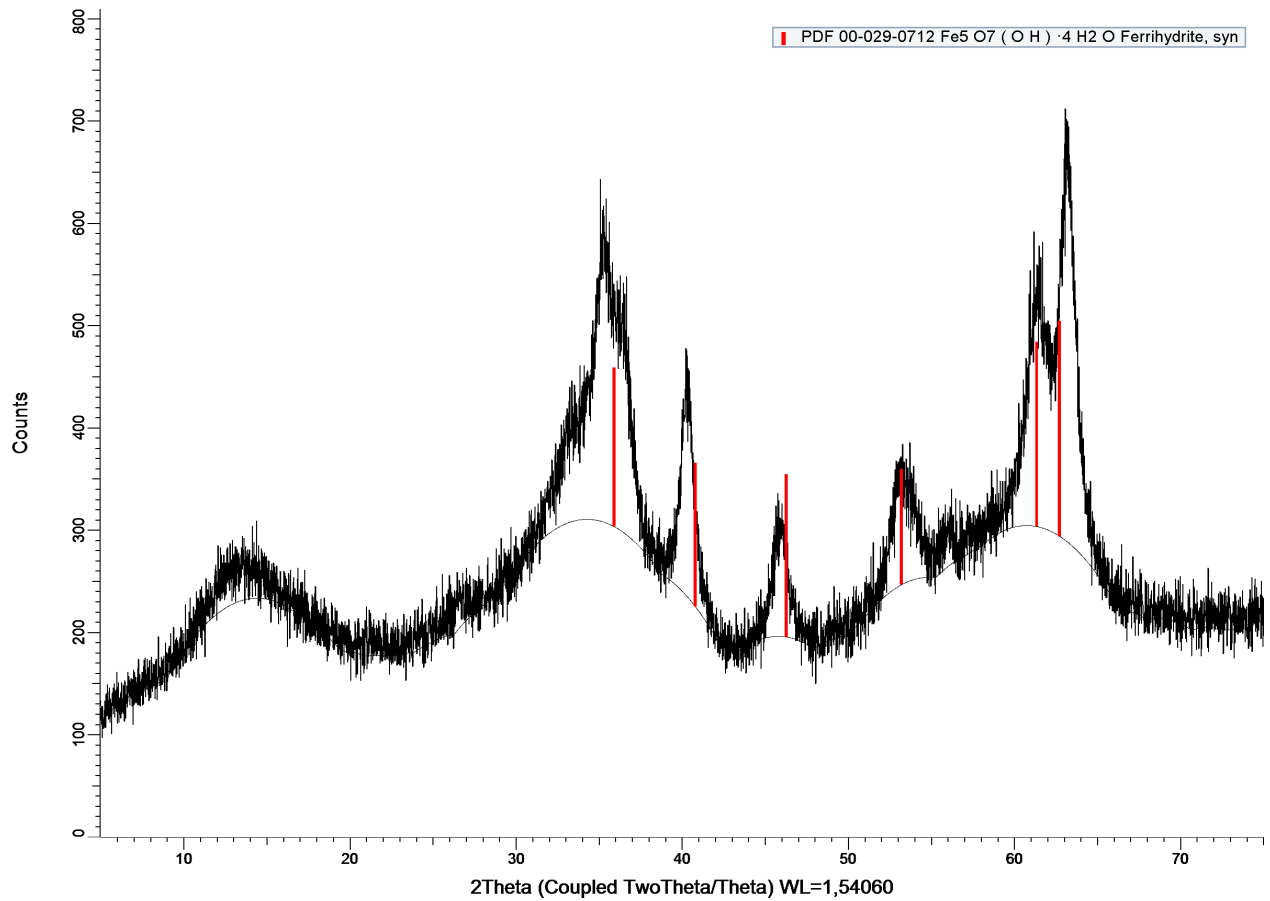
Figure B.1: XRD-spectra from experiment 1 performed at NTNU, 65°C with 45 min residence time, indicating ferrihydrite.
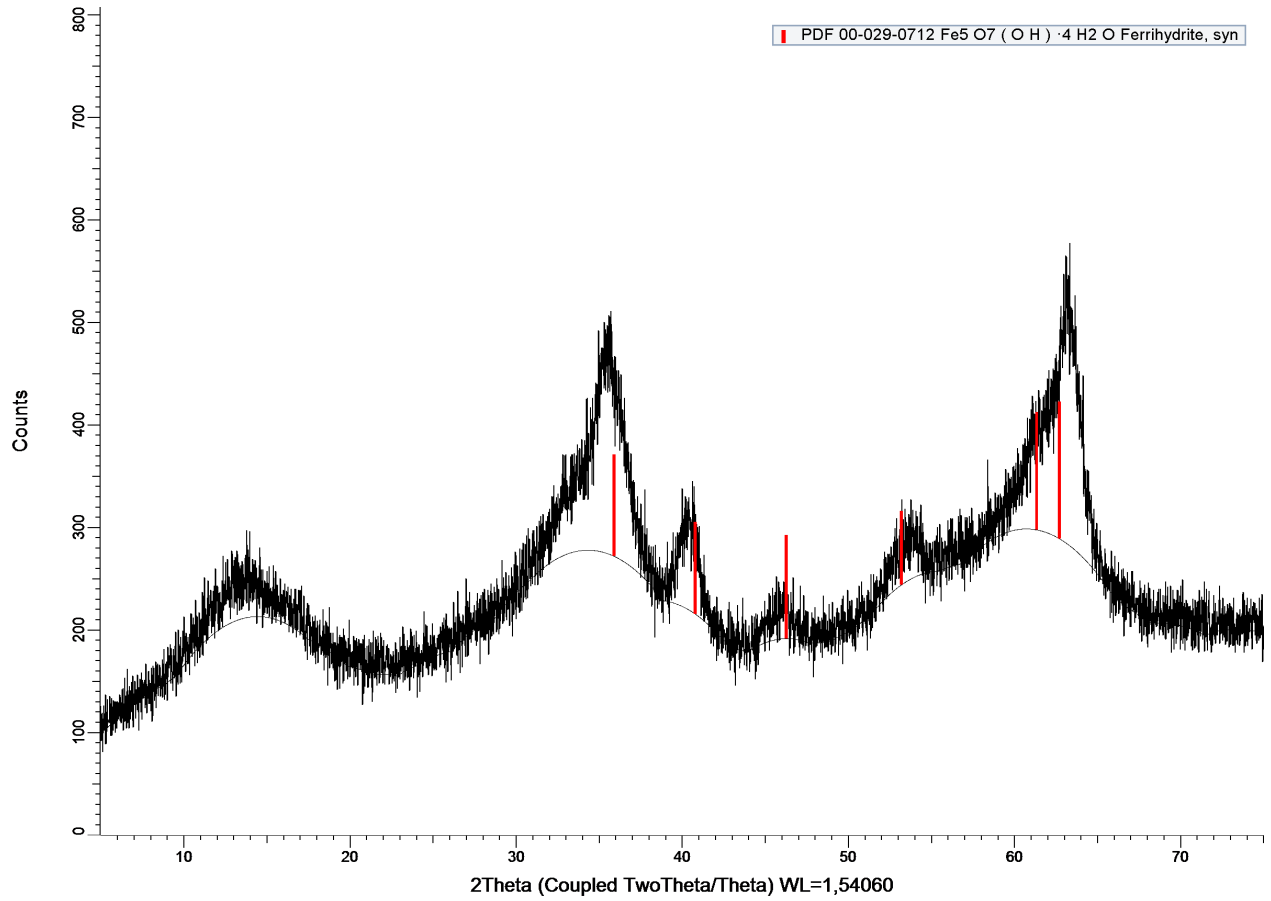
Figure B.2: XRD-spectra from experiment 2 performed at NTNU, 65°C with 45 min residence time, indicating ferrihydrite.
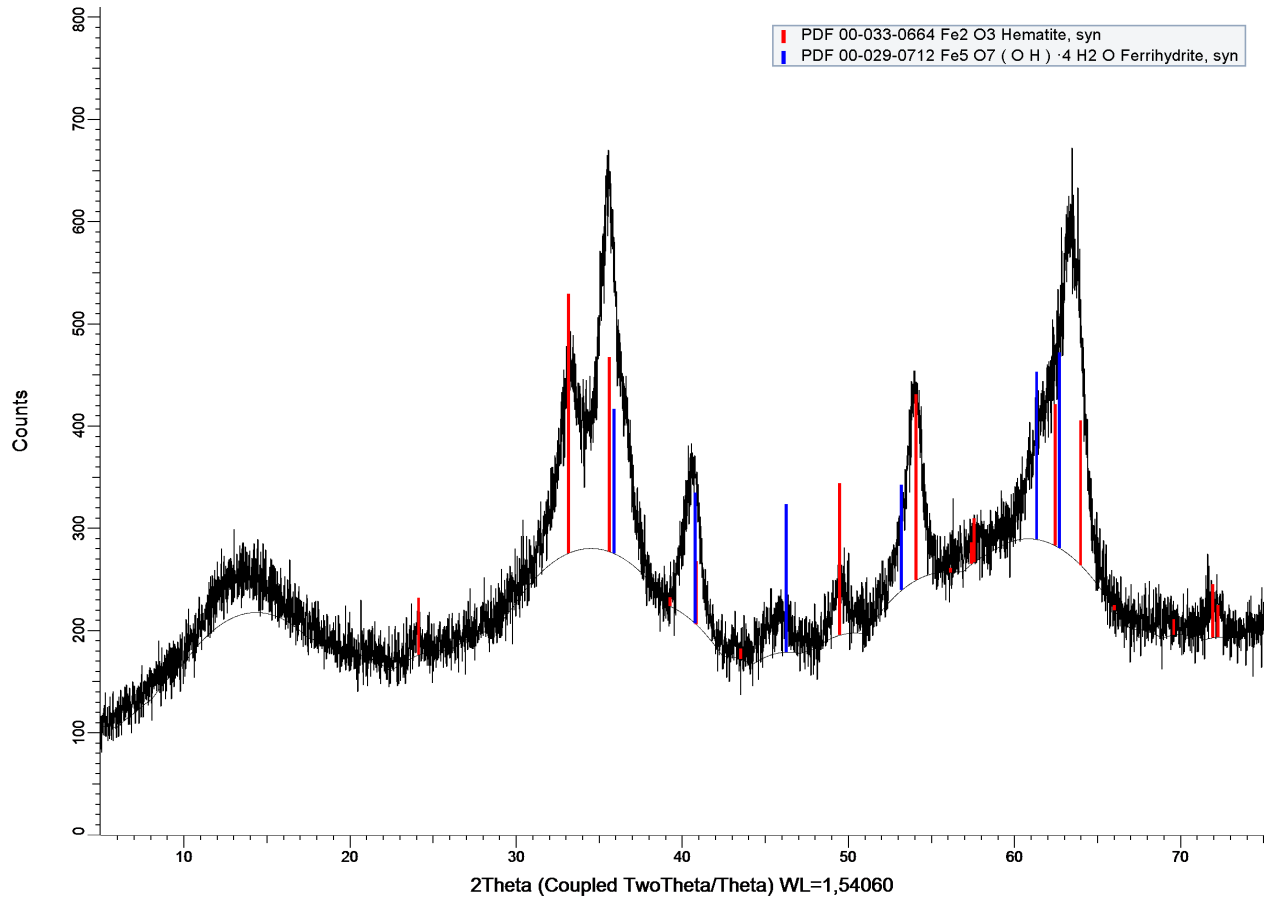
Figure B.3: XRD-spectra from experiment 3 performed at NTNU, 65°C with 45 min residence time, indicating ferrihydrite and/or hematite.
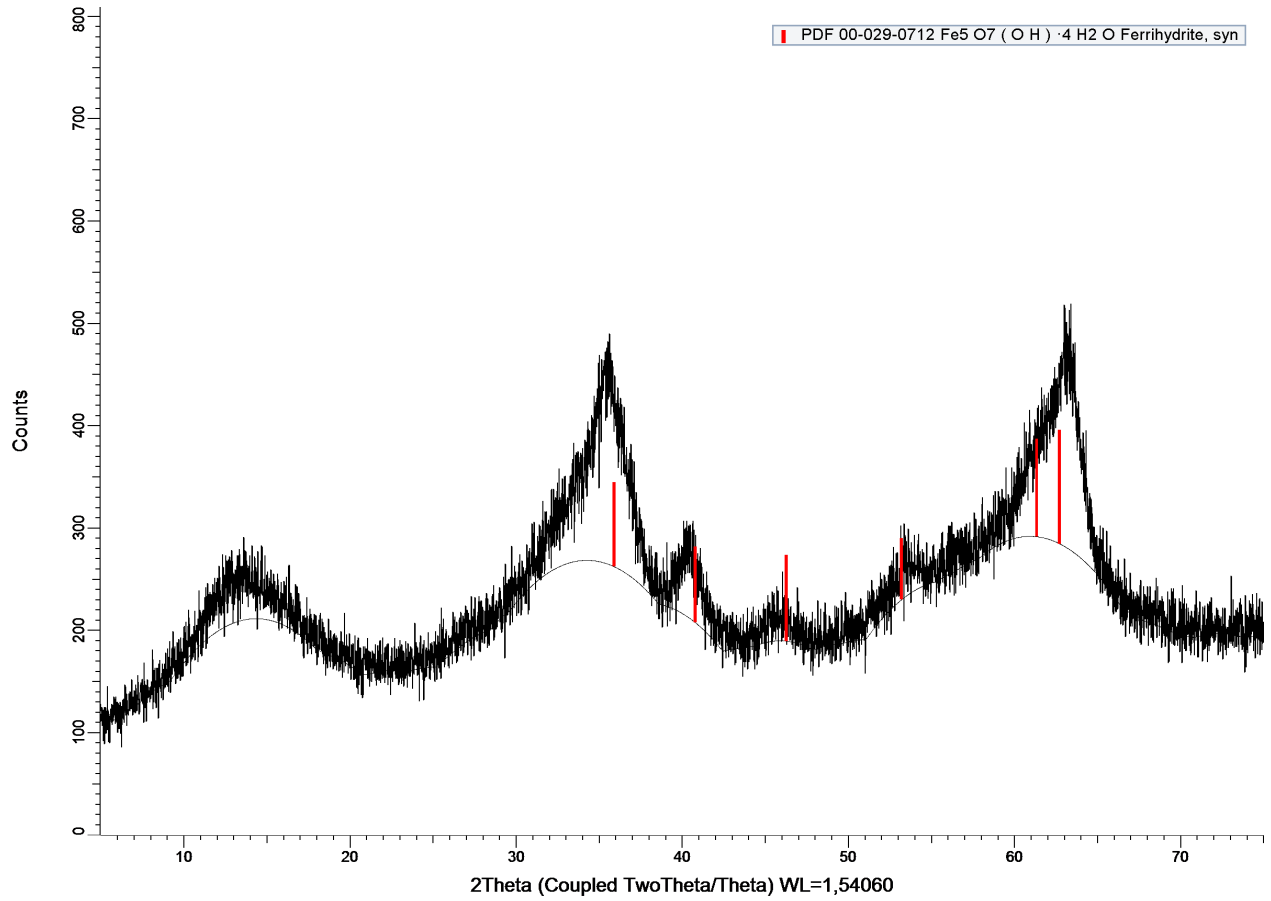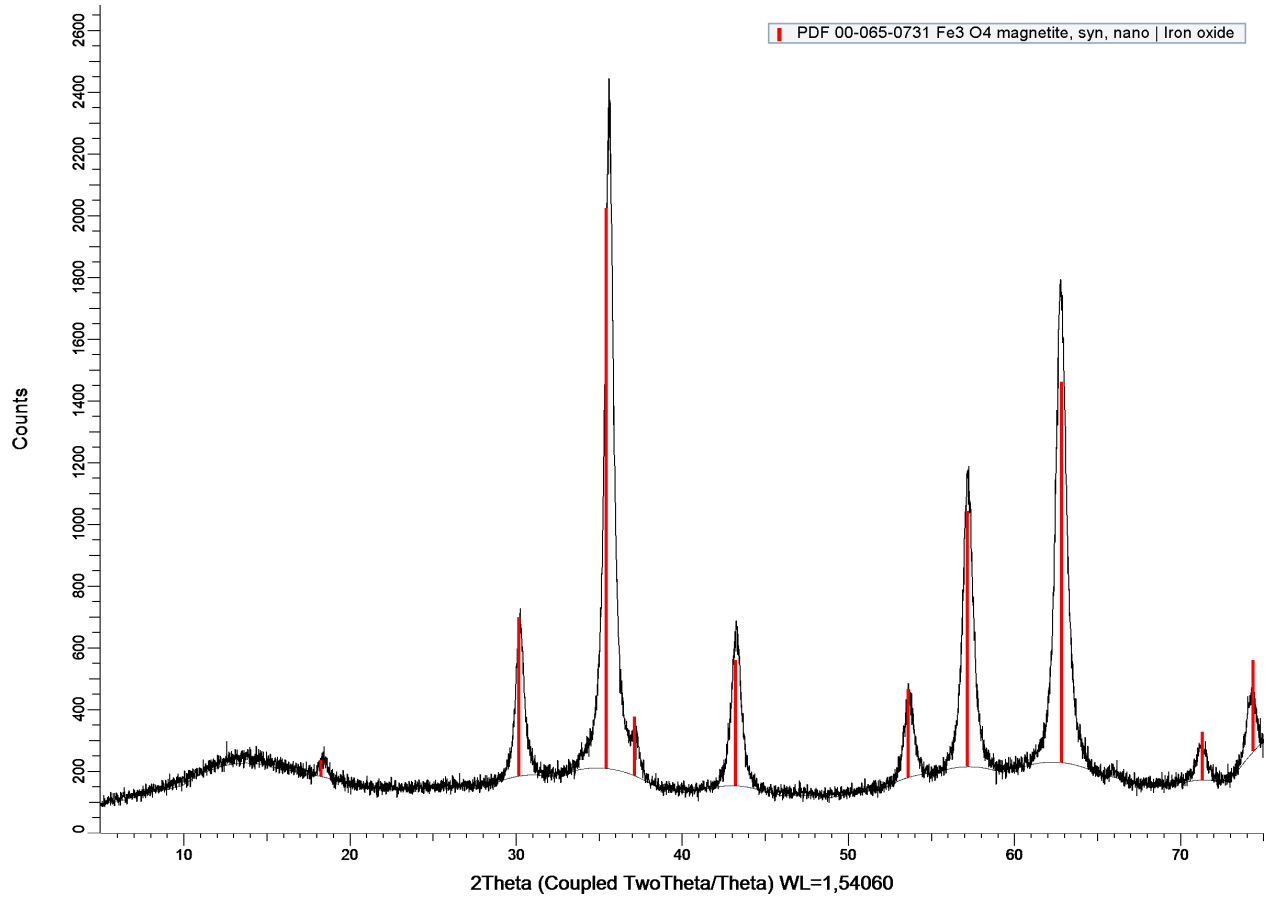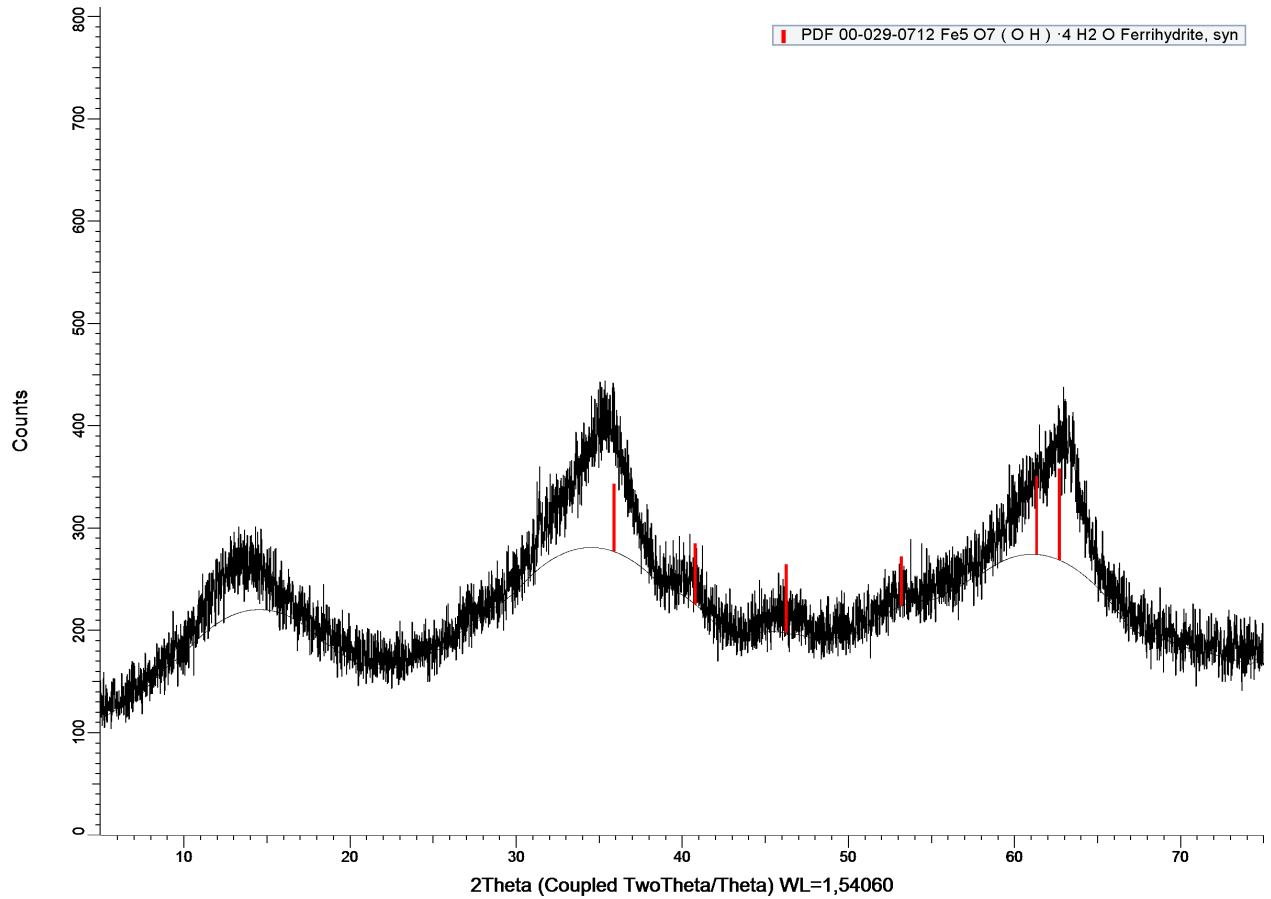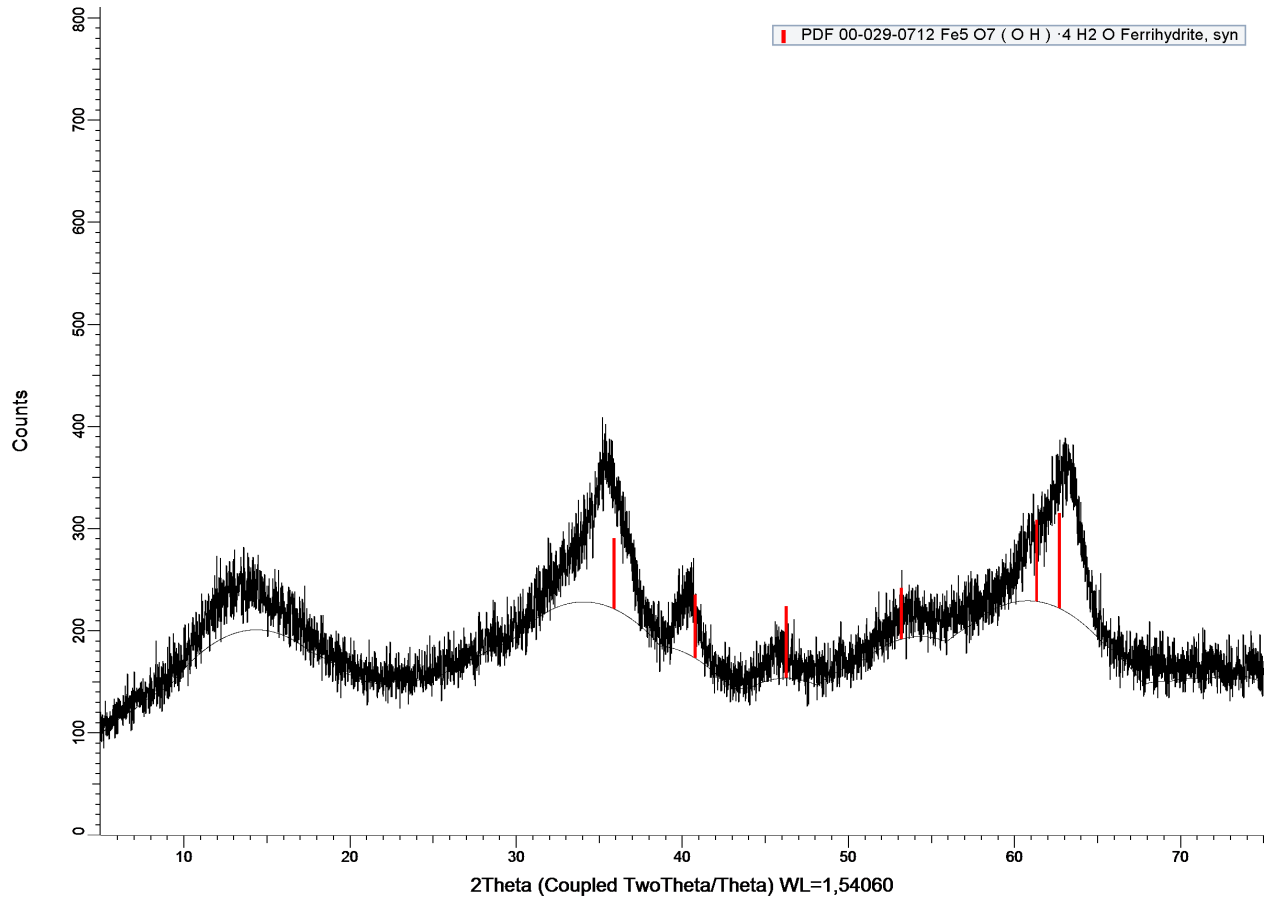
Figure B.4: XRD-spectra from experiment 4 performed at NTNU, 65°C with 15 min residence time, indicating ferrihydrite.

Figure B.5: XRD-spectra from experiment 5 performed at NTNU, 29°C with 15 min residence time, indicating magnetite.

Figure B.6: XRD-spectra from experiment 6 performed at NTNU, 29°C with 15 min residence time, indicating ferrihydrite.

Figure B.7: XRD-spectra from experiment 7 performed at NTNU, 79°C with 15 min residence time, indicating ferrihydrite.
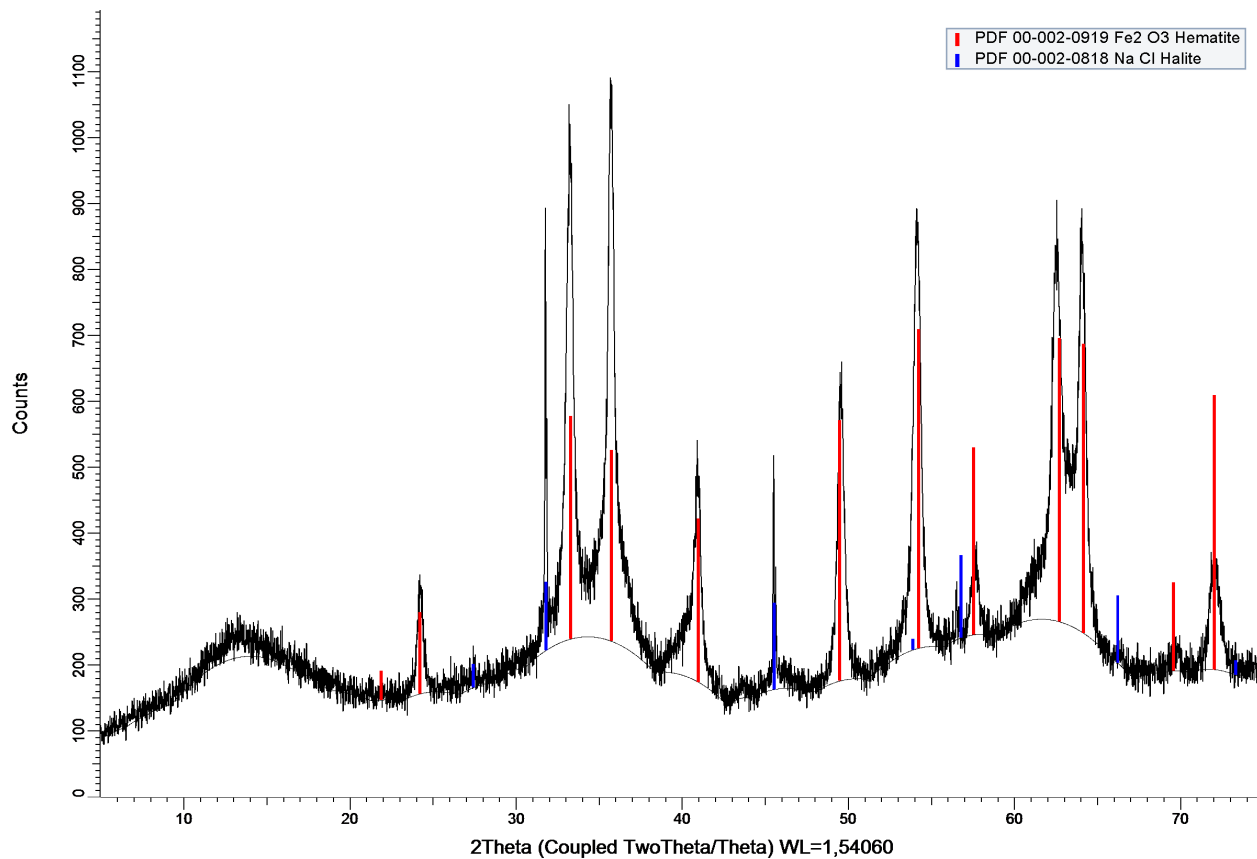
Figure B.8: XRD-spectra from experiment 7.2 performed at NTNU, batch after experiment 7, 90°C in 18.5 hours, indicating hematite. NaCl is also indicated because the sample was not washed during the filtration process.
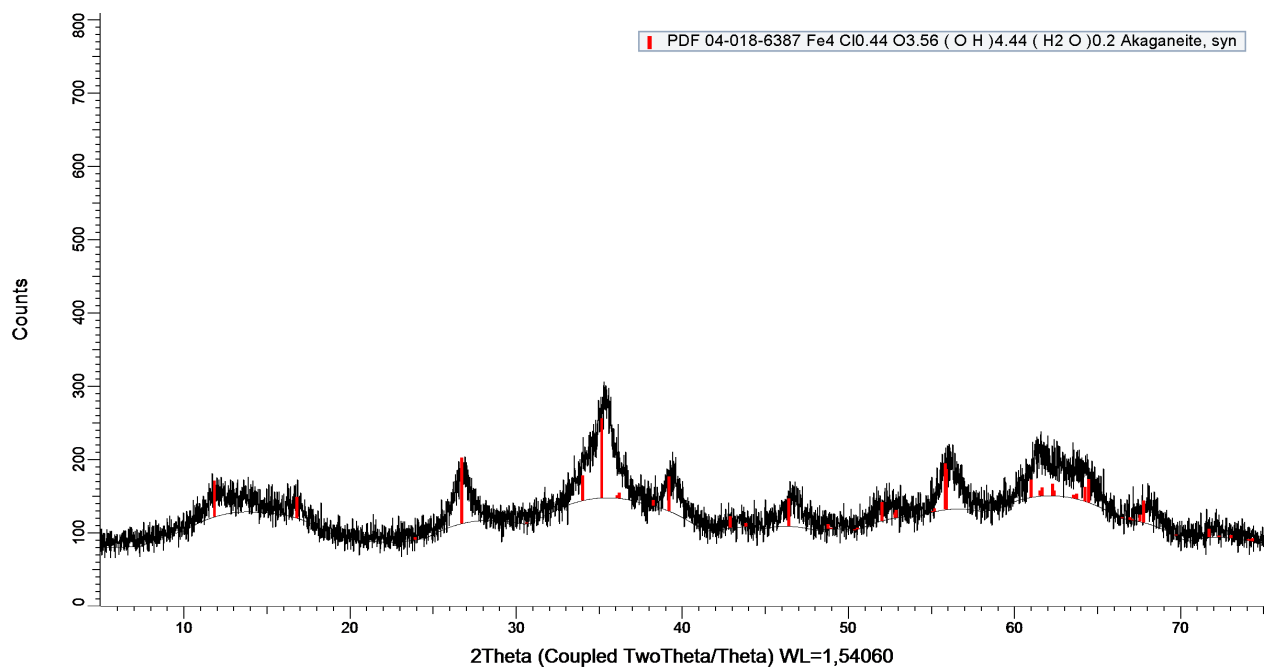
Figure B.9: XRD-spectra from test experiment performed at NTNU, at 25°C with pH 2.6 where the residence time of 45 min was ran for 7 times, indicating akaganeite.

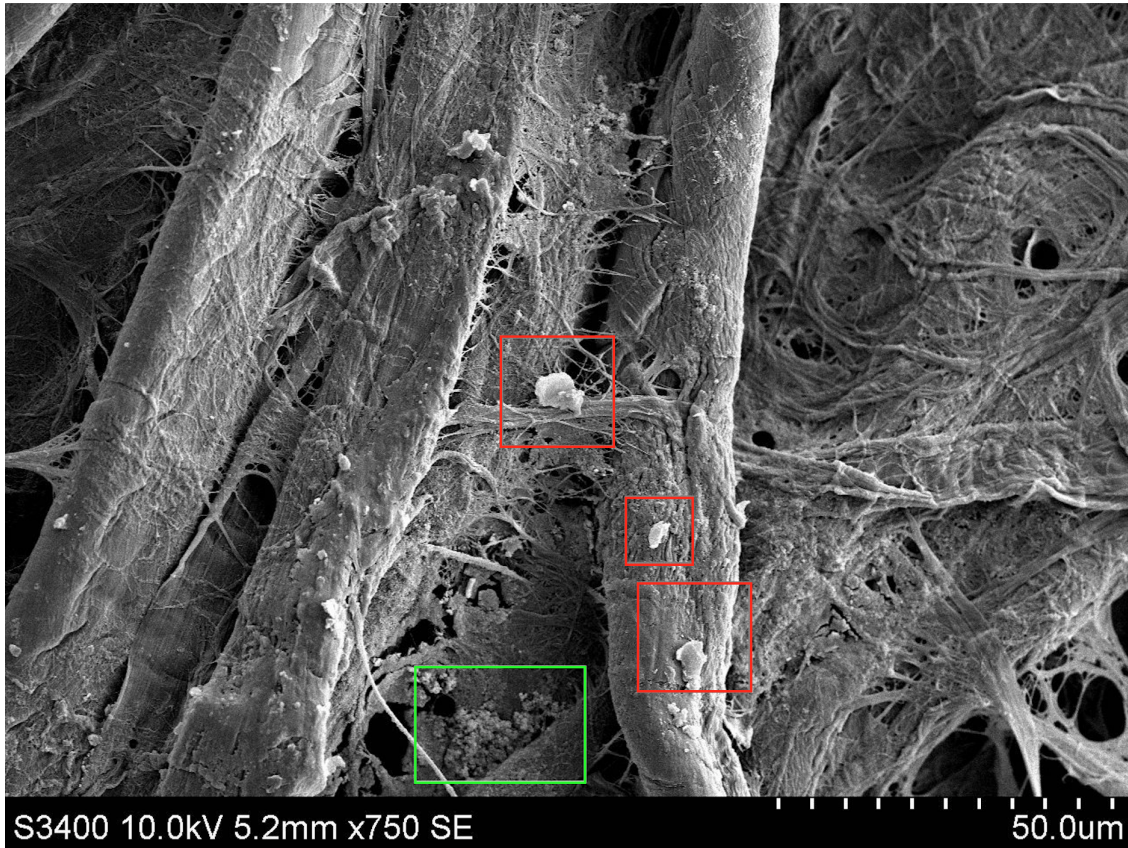# C   SEM Images from Experiments Performed at NTNU

Figure C.1: SEM image of experiment 5 performed at NTNU, 29°C with 15 min residence, with a defect pump in the end of the experiment resulting in magnetite. Red area may indicate magnetite formation and green area may indicate that there was still some ferrihydrite in the suspension. The background is fibers from the filter paper.
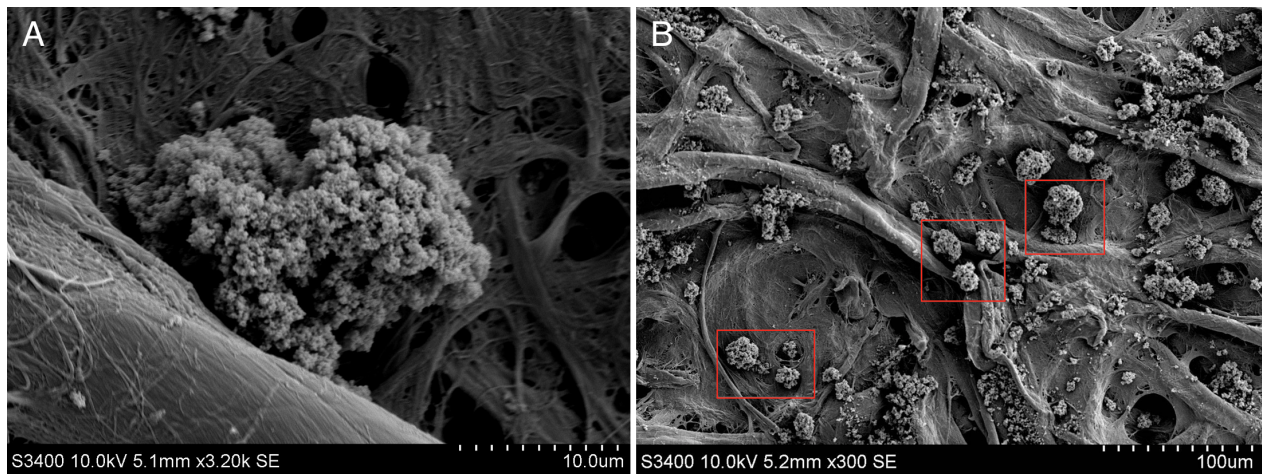
Figure C.2: SEM images of experiment 7 performed at NTNU, 79°C with 15 min residence time. A: A close up picture of a ferrihydrite bulk particle. B: Examples of ferrihydrite bulk particles marked in red. The background is fibers from the filter paper.

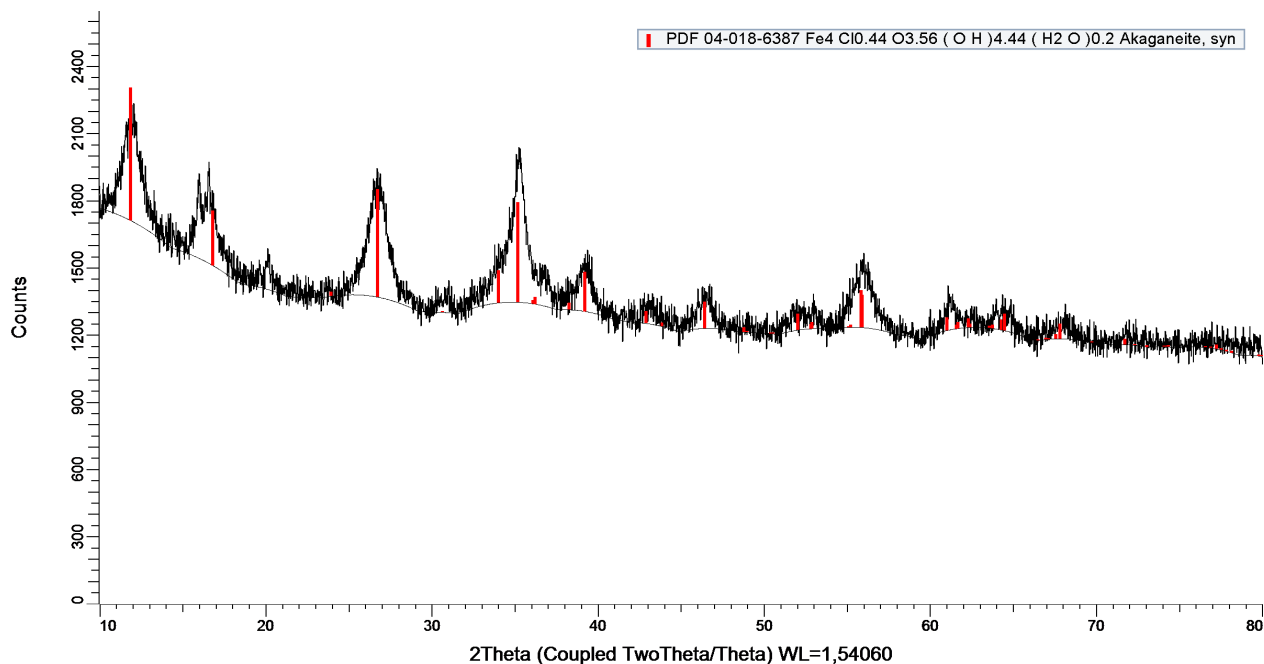# D   XRD-specters from Experiments Performed at Glencore

Figure D.1: XRD-spectra from experiment 1 performed at Glencore, 65°C with 75 min residence time, indicating akaganeite. Analyzed at Elkem.
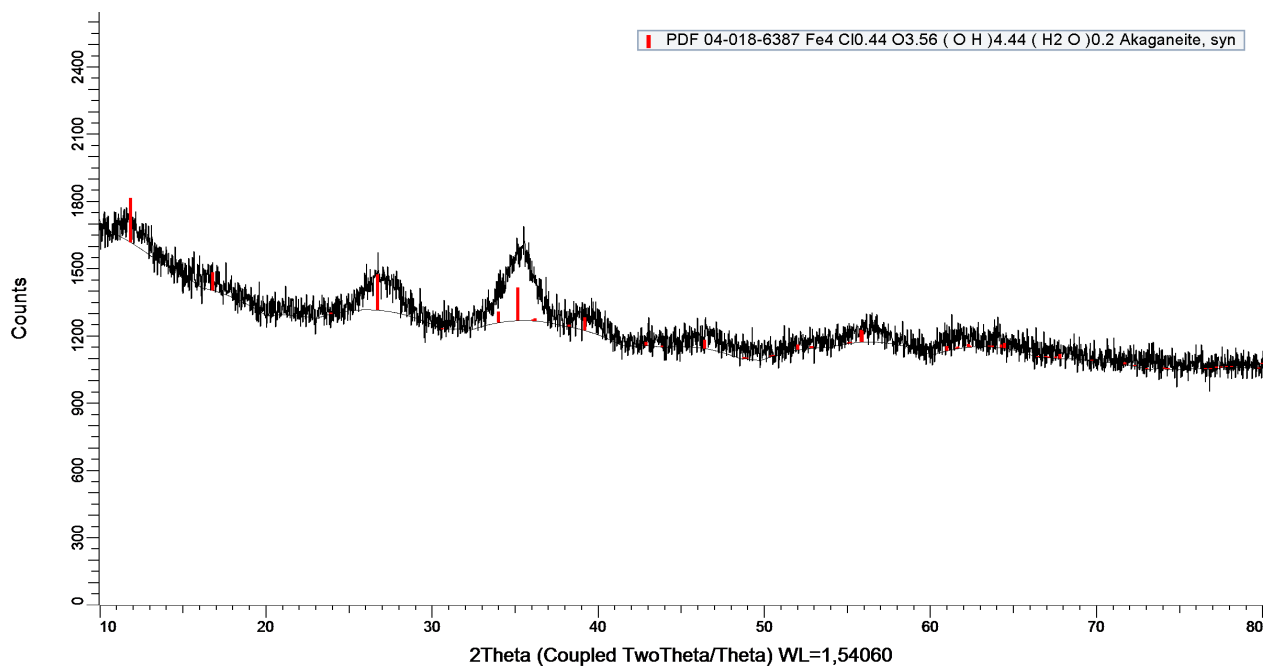
Figure D.2: XRD-spectra from experiment 2 performed at Glencore, 30°C with 75 min residence time, indicating akaganeite with the lowest intensity of the experiments. Analyzed at Elkem.
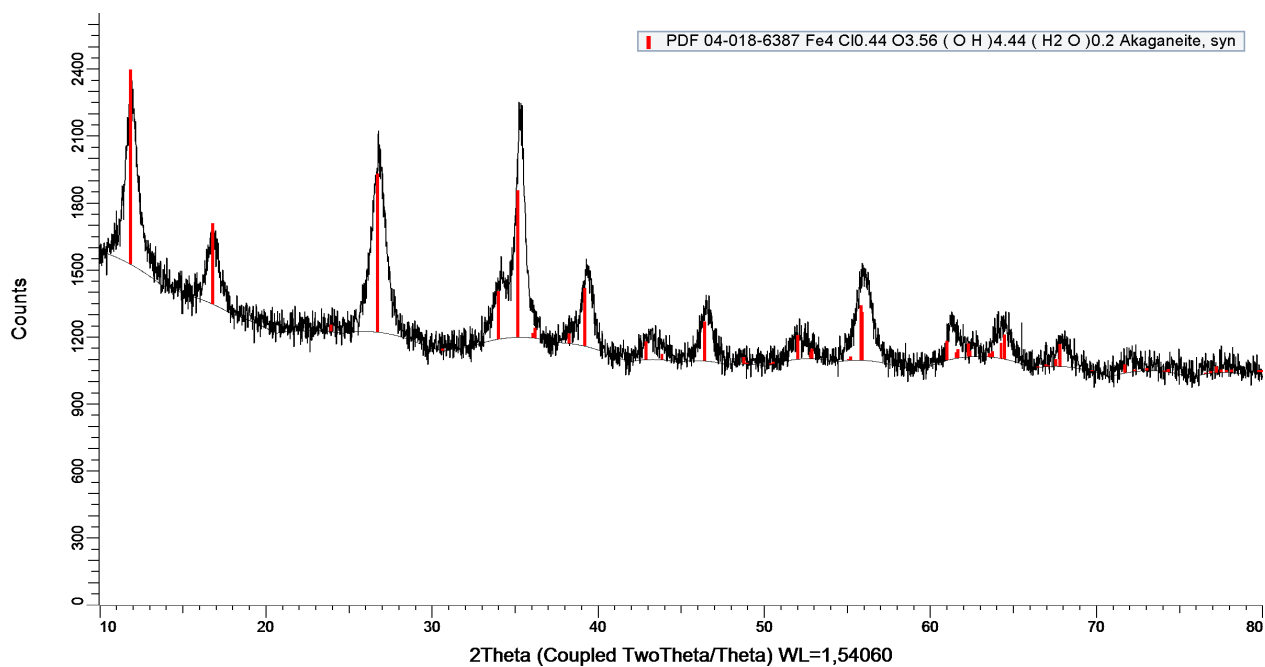

Figure D.3: XRD-spectra from experiment 3 performed at Glencore, 90°C with 75 min residence time, indicating akaganeite with the highest intensity of the experiments. Analyzed at Elkem.
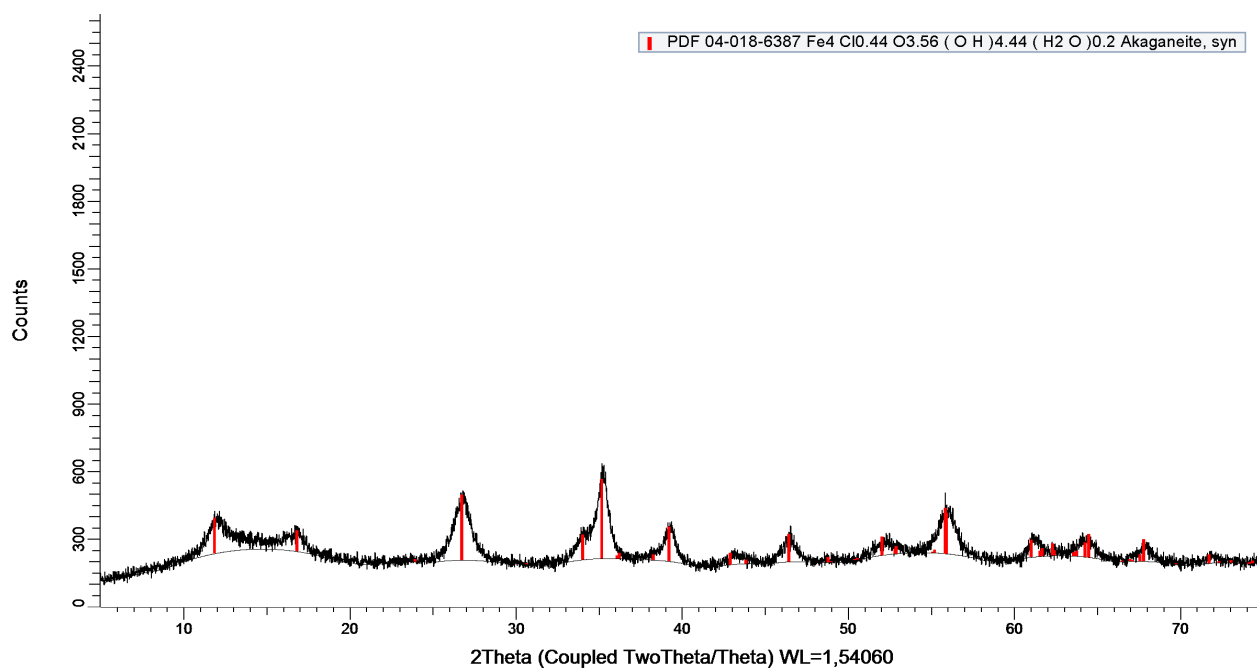
Figure D.4: XRD-spectra from experiment 4 performed at Glencore, 65°C with 45 min residence time, indicating akaganeite.
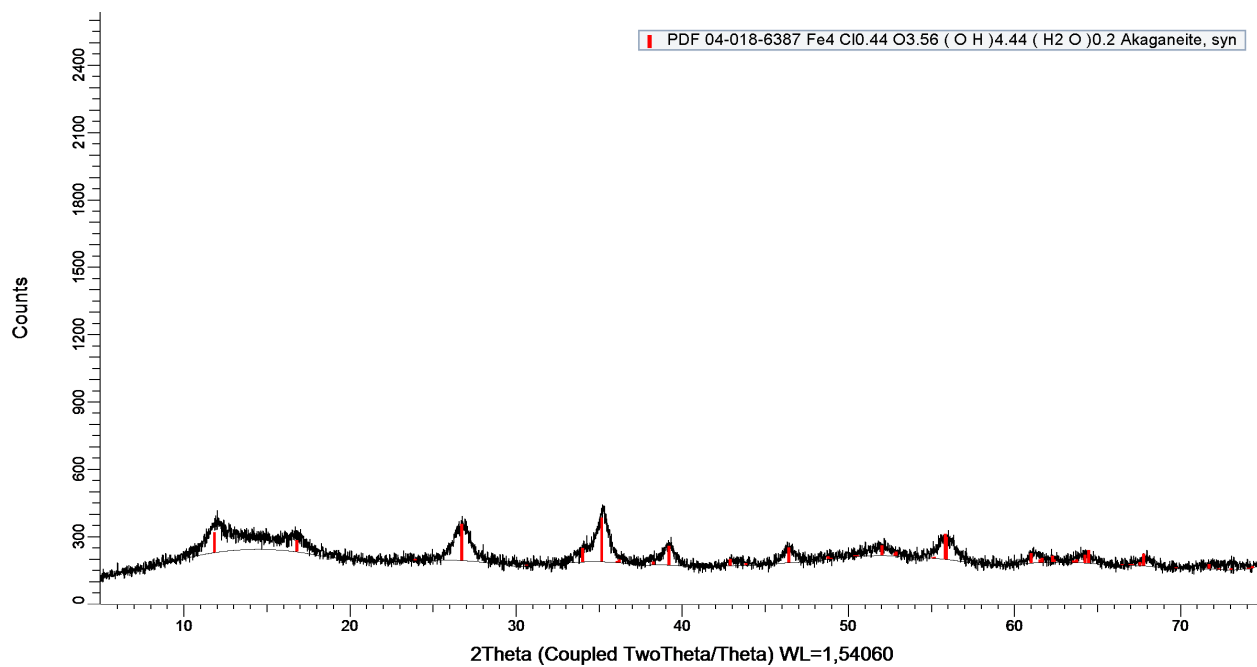

Figure D.5: XRD-spectra from experiment 5 performed at Glencore, 65°C with 75 min residence time, indicating akaganeite.

E   Calculations

E.1   Amount of Chemicals

Iron:

- Desired total iron concentration: 10 g/L
- Molecular weight iron: 55.845 g/mole
- Based on this the iron concentration was: 0.179 mole/L
- Molecular weight of the divalent iron chloride tetrahydrate used: 198.81 g/mole
- This demands an amount of divalent iron chloride tetrahydrate:

    0.179 mole/L · 198.81 g/mole = 35.6 g/L

Sodium hydroxide:

- Desired NaOH concentration: 0.35 mole/L
- Molecular weight NaOH: 40 g/mole
- This demand an amount of NaCl: 0.35 mole/L · 40 g/mole = 14.0 g/L

Hydrogen peroxide:

- Desired mole of H_2O_2 is 1:1 with mole of iron based on:
- $Fe^{2+} + H_2O_2 \rightarrow Fe^{3+} + HO^* + OH^-$
- Giving desired H_2O_2 concentration: 0.179 mole/L
- Molecular weight H_2O_2: 34.01 g/mole
- This demands an amount of 30 wt% H_2O_2: $\frac{0.179 mole/L \cdot 34.01 g/mole}{0.30} = 20.3$ g/L

These concentrations of iron, sodium hydroxide and hydrogen peroxide were desired in the reactor. To calculate what the feed concentrations had to be to achieve these concentrations in the reactor based on the flow of each pump, the calculated concentrations had to be multiplied with $\frac{Total flow}{Flow of the stream}$.

E.2 Calculation Example of Supersaturation

The calculation of the supersaturation (S) was based on Equation 4. For experiment 1 at NTNU the values are:

$[Fe^{3+}] = 43.59$ mg/L

$[OH^-] = 10^{-pOH} = 10^{-(14-pH)} = 10^{-(14-2.7)}$

$= 5.01 \cdot 10^{-12} mole/L \cdot 17g/mol \cdot 10^3 mg/g = 0.0000001$ mg/L

The activities were calculated using the Visual MINTEQ computer program based on the concentrations of ions and temperature. Ksp value for ferrihydrite is 10^{-38} [4].

$a_{Fe^{3+}} = 1.70 \cdot 10^{-6}$

$a_{OH^-} = 2.90 \cdot 10^{-10}$

$S = \left(\frac{1.70 \cdot 10^{-6} \cdot (2.90 \cdot 10^{-10})^3}{10^{-38}} \right)^{\frac{1}{4}} = 8$

E.3   Calculation Example of Cake Resistance

The calculation of cake resistance (α) was based on Equation 7, 8 and 9. The density of the solids ρ_s was set to 3.96 g/cm^3 for ferrihydrite [4]. The filtrate was considered as a sodium chloride solution, so the viscosity of the filtrate μ was set to 0.9286 $mPa \cdot s$ for 0.5 mol/kg NaCl aqueous solution at 25°C and 0.1 MPa [25]. For experiment 1 at NTNU the values are:

$$\epsilon = \frac{20cm^2 \cdot 0.5cm - \frac{0.74g}{3.96g/cm^3}}{20cm^2 \cdot 0.5cm} = 0.981$$

$$c = \frac{1.006g/cm^3}{\frac{1}{0.004} - \left(1 + \frac{1.006g/cm^3}{3.96g/cm^3} \cdot \frac{0.981}{(1-0.981)}\right)} = 0.004 \ g/cm^3$$

Where the mass fraction of solids is 0.004 in the formula.

$$\alpha = \frac{2 \cdot (20cm^2)^2 \cdot 200000000mPa \cdot 0.0057s/cm^6}{0.004g/cm^3 \cdot 0.9286 \ mPa \cdot s} = 2.48 \cdot 10^{11} \ \text{cm/g} = 2.48 \cdot 10^{11} \ \text{cm/g}$$

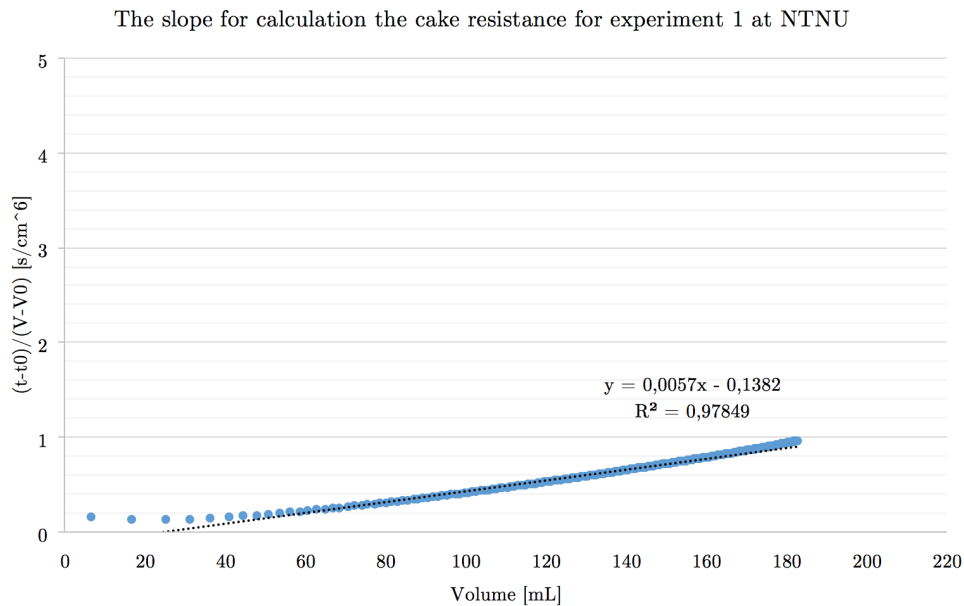Where 0.0057 s/cm^6 in the formula is the slope when plotting $\frac{t-t_i}{V-V_i}$ by $(V+V_i)$ in Figure E.1.

Figure E.1: $\frac{t-t_i}{V-V_i}$ plotted by $(V+V_i)$ for experiment 1 at NTNU, showing the slope of 0.0057 s/cm^6 used to calculate the cake resistance.

At Glencore the viscosity of the filtrate was measured by using viscometer.

A visualization of the filterability by time for experiment 1 at NTNU is given in Figure E.2.

It can be seen that the volume of the filtrate decreases with time, which agree with the theory presented in section 2.6. It is stated that the rate of filtration decreases with increasing cake thickness when performing cake filtration.
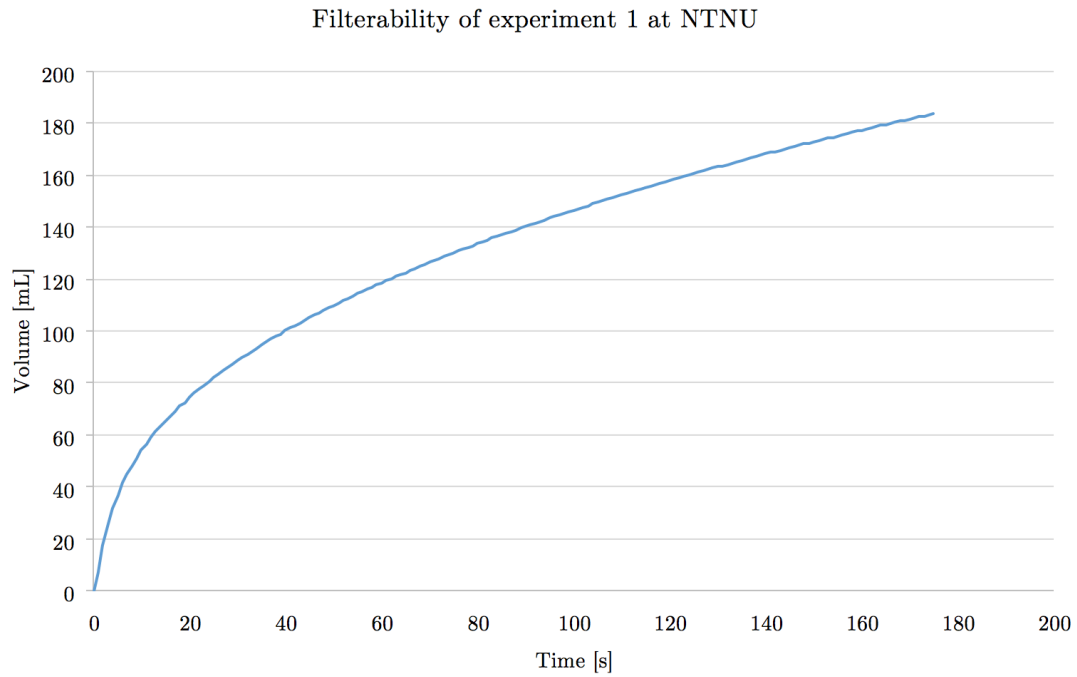

Figure E.2: Volume plottet against filtration time for experiment 1 at NTNU.

E.4   Calculation of Standard Deviation for Experiments at NTNU

Results from the filtration:

- $7.24 \cdot 10^{13}$ m/kg

- $6.37 \cdot 10^{13}$ m/kg

- $6.26 \cdot 10^{13}$ m/kg

- $6.10 \cdot 10^{13}$ m/kg

- $6.40 \cdot 10^{13}$ m/kg

- Sample mean: $6.47 \cdot 10^{13}$

Standard deviation: Sd$=\sqrt{\left(\frac{\sum (x-x_{av})^2}{(n-1)}\right)} = 4.43 \cdot 10^{12}$ Calculated using STDAV.S in Excel.

Relative standard deviation: $\frac{100 \cdot Sd}{Mean} = 6.9\%$

F Procedures

F.1 Filtration Procedure

A filter paper with area of 20 mm^2 was cut out of A4 filter papers, type Pennevis PA 1196 B Multi/Multi 4 L/dm^2 per min @ 20 mmWC, and attached in the bottom of the filtration unit, suspension (200 mL) was filled into the column and the top part of the unite was attached. The filtration was performed with suspensions at 25°C to have equal conditions at the filtration, despite experimental temperature. The pressure was 2 bar using nitrogen gas. The height of the filter cake was measured by using a customized ruler. The filter cakes were dried for 48 hours.

F.2 UV-vis Procedure

The buffer solution used to determine amount of Fe^{3+} was made by sodium acetate tetrahydrate (280 g) and sulfosalicylic acid (40 g) diluted to 2 L. Concentrated hydrochloric acid (160 mL) was diluted to 2 L and added to the sulfosalicylic acid solution until pH 2.2 was reached, then diluted to a total of 4 L.

25 mL filtrate and 10 mL buffer solution were diluted to 100 mL and analyzed at 508 nm to find amount Fe^{3+}. To find total amount of Fe in the filtrate the same procedure was performed in addition to add two droplets of 3% H_2O_2.

The calibration curve used to convert absorbance to amount of iron is given i Figure F.1.

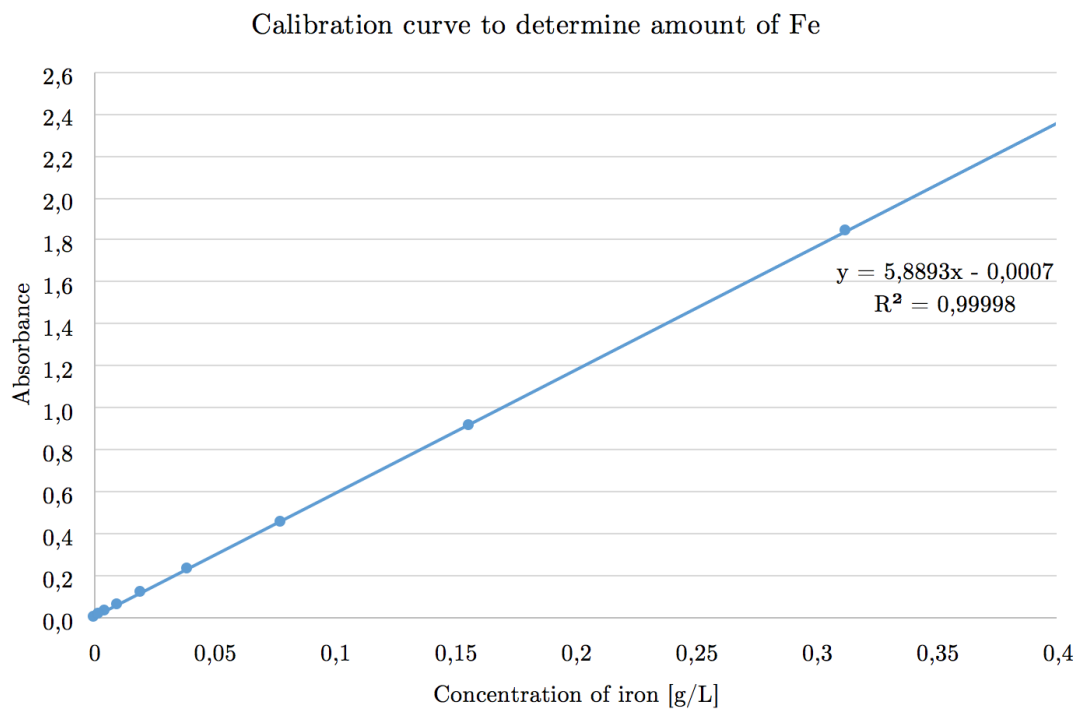Calibration curve to determine amount of Fe

$y = 5{,}8893x - 0{,}0007$

$R^2 = 0{,}99998$

Figure F.1: The calibration curve used to convert absorbance to amount of iron.

G Risk Assessment

Detaljert Risikorapport

ID	13414		**Status**	**Dato**
Risikoområde	Risikovurdering: Helse, miljø og sikkerhet (HMS)		Opprettet	30.09.2016
Opprettet av	Mona Aufles Hines		Vurdering startet	30.09.2016
Ansvarlig	Mona Aufles Hines		Tiltak besluttet	
			Avsluttet	

EEART, masterstudent, Mona Aufles Hines, 2016

Gyldig i perioden:

-

Sted:

Laboratorie K4, 1.etg.

Mål / hensikt

Hensikten med denne risikovurderingen er å se på risiko ved masteroppgaven.

Bakgrunn

Krystallisering i reaktor ved bruk av:
Dobbeltvegget reaktor (kontinuerlig)
Vannbad
Tørkeskap
Filtrering ved vakuum/trykk og filterpapir

Analysering ved:
SEM, PXRD, UVvis

Kjemikalier som brukes:
Sitronsyre
Natriumhydroksid
Jern(II)klorid
Jern(III)klorid
Hydrogenperoksid 30%
Fortynnet løsning av natrium☐acetat, sulfosalicylsyre, hydrogenklorid

Beskrivelse og avgrensninger

Jobber ikke med giftige kjemikalier, risikodatablad er gitt for aktuelle kjemikalier, ikke høyere temp. enn 80 grader, opplæring gitt på instrumenter.

Forutsetninger, antakelser og forenklinger

[Ingen registreringer]

Vedlegg

[Ingen registreringer]

Referanser

[Ingen registreringer]

Figure G.1: Front page of the risk assessment for this thesis.